BMC Biology

RESEARCH

Open Access

Major transitions in early coral development: novel insights enabled by visualisation of a comprehensive transcriptomic dataset for *Acropora millepora*

Ramona Brunner[1,2†], Mila Grinblat[1,2†], Aurelie Moya[1,2†], Sylvain Foret[3^], David C. Hayward[3], Bruno Lapeyre[1,4], Eldon E. Ball[3*], Ira Cooke[2,5] and David J. Miller[1,2*]

Abstract

Background Given the ecological importance of reef-building corals (Scleractinia), it is perhaps surprising that the molecular mechanisms underlying many of the morphological and metabolic changes during their development remain unclear. In part, this is due to the lack of a comprehensive transcriptomic dataset for any coral. A second challenge in the analysis of such non-model developmental datasets is that the volume of data often complicates its interpretation.

Results To overcome these limitations, we profiled gene expression in *Acropora millepora* across 26 life stages from unfertilised eggs to juvenile polyps and developed an interactive online tool based on the R-application Shiny to simultaneously visualise changes in the expression of large numbers of genes. As expected, major transcriptomic changes (transitions) occurred during gastrulation and the acquisition of competence. Surprisingly, however, settlement triggered by using an extract of the natural inducing crustose coralline alga did not immediately lead to major changes in gene expression, but a major transition involving many genes was observed 3–6 h after settlement induction.

Conclusions We hope that providing access to this extensive developmental transcriptome dataset and software to facilitate its analysis will expedite a better understanding of the changes that occur during coral development. The online tool is available at https://amil-deview.mmb.group.

Keywords Maternal-zygotic transition, Juvenile-adult transition, Metamorphosis, Coral development, Larval settlement

†Ramona Brunner, Mila Grinblat and Aurelie Moya contributed equally to this work.

^Sylvain Foret is deceased. This paper is dedicated to his memory.

*Correspondence:
Eldon E. Ball
eldon.ball@anu.edu.au
David J. Miller
david.miller@jcu.edu.au
Full list of author information is available at the end of the article

Background

Broadcast spawning corals, such as *Acropora* spp., release buoyant eggs and sperm and fertilisation occurs in the water column [1–3]. The early developmental stages are planktonic, ultimately reaching a motile stage known as a planula larva which becomes "competent"—that is, it becomes capable of settlement and metamorphosis—after a period of development of variable duration [4] (Fig. 1). Competence is marked by a change in behaviour, from horizontal swimming to swimming into the substratum and testing it for chemical cues. In nature, the settlement of competent larvae generally involves selection of appropriate sites, based on perception of a range of cues that include small molecules, at least some of which are produced by bacteria associated with substrate biofilms and algae (e.g. [5–8]). The quality and nature of available light also play a part in settlement site selection in the case of many reef-building corals [9–11].

Various aspects of early coral development have previously been studied at the transcriptome level, with the initial focus being characterisation of individual genes homologous to those playing key developmental roles in bilaterians [15–18]. The first larger-scale analyses were based on microarrays [12, 19, 20], 454 GSFlx sequencing [21], SOLiD sequencing [22] or subtractive hybridisation [13]. Whilst Reyes-Bermudez & Rodriguez-Cabal [23] used microarray technology to compare gene expression profiles across the planula/polyp divide and adult *Acropora millepora*, most recent studies have used high-throughput DNA sequencing technologies to characterise specific developmental stages. Much of this work has focussed on members of the Acroporidae (genera *Acropora* and *Montipora*), with sampling regimes designed to address specific questions. For example, Takeuchi et al. [24] and Ishii et al. [25] investigated the processes of calcification and commitment to metamorphosis in *Acropora* spp., respectively. van Etten et al. [26] compared egg and sperm transcriptomes of *Montipora capitata*, and Chille et al. [27] concentrated on gene expression changes in the same species during the maternal/zygotic transition (MZT). Similar questions have also been addressed in *Porites asteroides* (Mansour et al. [28] and Walker et al. [29]), which belongs to a distinct family of complex corals. The recent developmental study on *M. capitata* by Huffmyer et al. [30] represents an important advance in that transcriptomic data were supplemented with metabolomic analyses to investigate the nutritional shift from maternal lipids to symbiont photosynthates in this vertically transmitting coral. Much higher cellular resolution expression datasets are becoming available for scleractinians [31–33], but so far these have been limited to a few developmental stages. Table 1 summarises recent publications on the

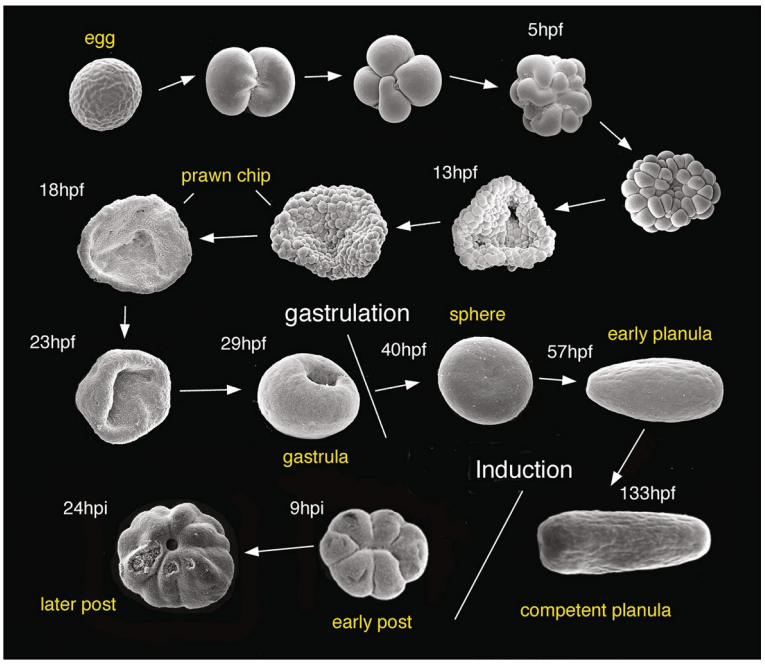

Fig. 1 SEM images summarising the morphological changes that occur during early development of *Acorpora millepora*. Times are given in hours post fertilisation (hpf) or hours post induction (hpi) and are typical for ambient temperatures of around 26 °C. Major developmental stages are labelled and places in the developmental sequence of two major events, gastrulation and induction with a settlement cue, are indicated. Some of the SEM images have been previously published in Grasso et al. [12], Hayward et al. [13], and Ball et al. [14]

Table 1 Previous studies on the gene expression in early development of hard corals

Coral species	Stages sampled				Focus of study	Methodology
	Pre-planula	Planula	Post-settlement	Adult		
Acropora millepora						
Grasso et al., 2008 [12]	8 hpf (prawn chip)	83 hpf	130 hpf	Adult	Early survey of developmental changes	EST arrays
Grasso et al., 2011 [20]	-	-	0.5 hpi 4 hpi 12 hpi	-	Metamorphosis	EST arrays
Hayward et al., 2011 [13]	-	Planula	Primary polyp	-	Pre vs post settlement	SSH
Strader et al., 2018 [4]	22 hpf 46 hpf	73 hpf 89 hpf 5–12 dpf in 24-h intervals	-	-	Competence and fluorescence	RNA-Seq
Reyes-Bermudez & Rodriguez-Cabal, 2024 [23]	-	96 hpf	144 hpf 192 hpf	Adult	Metamorphosis and calcification	EST arrays
Acropora digitifera						
Takeuchi et al., 2016 [24]	Egg Blastula Gastrula	Planula	Primary polyp	Adult	Calcification genes	RNA-seq
Reyes-Bermudez et al., 2016 [34]	12 hpf (prawn chip) 24 hpf (gastrula) 48 hpf (sphere)	96 hpf	-	Adult	Stage-specific transcript profiles	RNA-seq
Acropora tenuis						
Ishii et al. 2022 [25]	-	0 hpi	1 hpi 6 hpi	-	Commitment to settlement	RNA-seq
Montipora capitata						
Van Etten et al., 2020 [26]	Egg Sperm	-	-	-	Comparison of egg and sperm transcriptomes	RNA-Seq
Chille et al., 2021 [27]	0 hpf (unfertilised egg) 1 hpf (fertilised egg) 4 hpf (cleavage) 9 hpf (prawn chip) 14 hpf (early gastrula) 22 hpf (mid gastrula) 1.5 dpf (late gastrula)	9 dpf	-	Adult	Maternal-zygotic transition	RNA-Seq
Huffmyer et al., 2025 [30]	1 hpf (fertilised egg) 5 hpf (cleavage) 38 hpf (late gastrula) 65 hpf (late gastrula)	93 hpf 163 hpf 183 hpf	183 hpf 231 hpf	-	Metabolism during early development	RNA-Seq
Porites asteroides						
Mansour et al., 2016 [28]	-	Pre-settlement	Post-settlement	Adult	Calcification, settlement and symbiosis	RNA-Seq
Walker et al., 2019 [29]	-	Pre-competent, competent planula	-	-	Compared non-probing and probing planulae	RNA-Seq
Montastrea faveolata						
Reyes-Bermudez et al., 2009 [19]	-	Planula	Primary polyp	Adult	Metamorphosis and onset of calcification	EST arrays
Stylophora pistillata						
Levy et al., 2021 [31]		Planula	Primary polyp	Adult	Characterisation of single cell types	RNA-Seq

molecular bases of coral development, including the primary focus of each of these studies.

To address the need for a comprehensive transcriptomic dataset, we profiled gene expression of *Acropora millepora* across 26 life stages from fertilised eggs to juvenile polyps and developed an interactive online tool based on the Shiny web framework to visualise changes in the expression of groups of genes. We present an

overview of the data, focussing on major transitions in gene expression and on processes not previously investigated, but hope that further exploration of the dataset via the website facilitates progress towards solutions for the crises currently faced by coral reefs worldwide. Our study also reveals the importance of combining spatial expression data, as revealed by in situ hybridisation, with the data obtained by RNAseq, in order to better understand gene function.

Results

Major transcriptional transitions visualised using DEView

During the development of *A. millepora*, the period immediately following fertilisation (0–5 h) was characterised by rapid rounds of cell division (Fig. 1) accompanied by relatively limited changes in gene expression (Fig. 2), implying that this phase is driven largely by maternal mRNAs and proteins. After that time, more extensive changes in gene expression occurred resulting in resolvable PCA clusters. After completion of gastrulation at 35hpf, embryos were spherical and became motile at 45hpf. Elongation from pear- (57hpf) to spindle-shaped larvae (69hpf) resulted in planulae that were not searching at 81hpf but were probing the environment for appropriate settlement sites at 93hpf, by which time they were competent to settle (Fig. 1). At 133hpf, settlement was induced with ethanolic extract of crustose coralline algae (CCA) but the 133hpf transcriptome data represent the untreated state. Settlement induction caused larvae to further elongate at 15mpi before forming disc-like shapes by contracting along the oral-aboral axis. Most larvae were metamorphosed at 2hpi and by 3hpi 100% of larvae had initiated metamorphosis, characterised by a six-fold symmetry around an oral pore in the centre. Whereas transcriptome data for the 0–3hpi stages clustered with those for late planula stages, data for 6–72hpi stages formed a discrete and well-resolved cluster (Fig. 2) during which metamorphosing polyps developed a 12-fold symmetry and formed tentacles around the oral opening. The polyp initiates calcification at the former aboral part, which becomes the calicoblastic ectoderm [35–37].

Differential gene expression analysis (Fig. 3) clearly highlights that, in addition to the expected early (13–35hpf) transcriptional events corresponding to zygotic genome activation, major transitions in gene expression also occurred at 81–133hpf and 3–6hpi. Differential gene expression analysis between consecutive timepoints was conducted by importing the RSEM results into DESeq2, considering the fertilisation cross and sampling time point in the design formula. Transcripts with less than 10 counts in less than or equal to 2 replicates (smallest number of replicates per timepoint) were removed. Differentially expressed transcripts were calculated using DESeq2 by specifying consecutive timepoints as contrasts and selecting an adjusted p-value ≤ 0.05.

The construction of weighted gene co-expression networks (WGCNA) [38], which group modules of genes according to correlation in their expression patterns, also

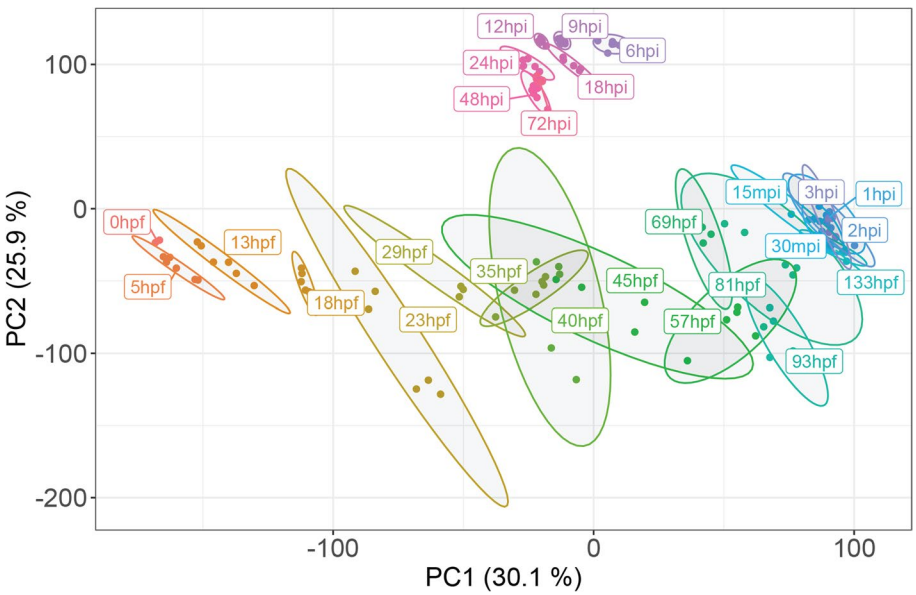

Fig. 2 PCA analysis of the developmental transcriptomic data. Principal component analysis (PCA) of the developmental transcriptome data with ellipses representing 95% confidence levels. At 93 h post fertilisation (hpf), larvae were competent to settle in response to ethanolic CCA extract and settlement was induced at the age of 133hpf. Settlement induction caused larvae to elongate at 15 min post induction (mpi) and 100% of larvae had initiated metamorphosis at 3 h post induction (hpi). A major change in gene expression occurred between 3 and 6hpi

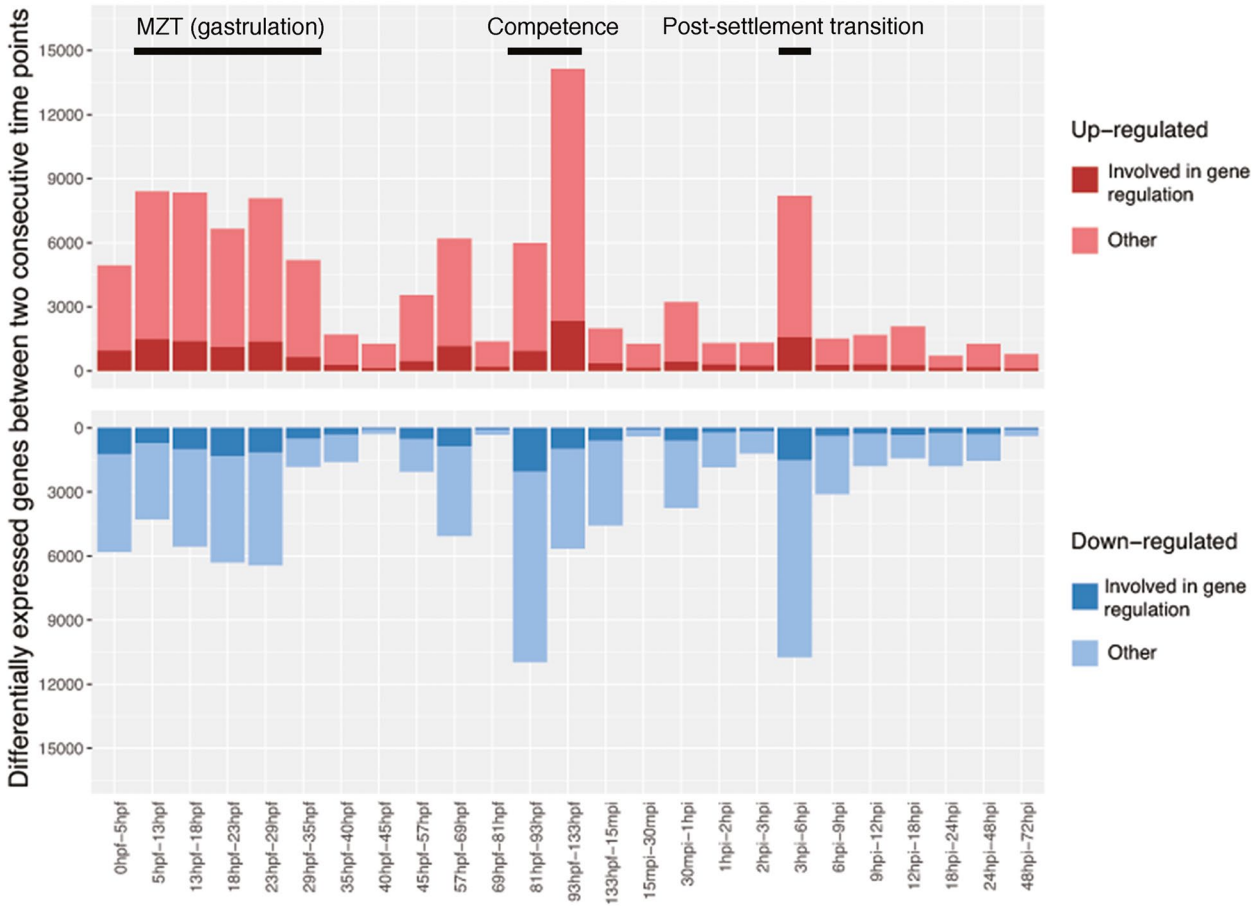

Fig. 3 Serial up-down expression plots reveal changes in gene expression between consecutive time points during development. There are three periods that show major changes in expression: early development leading up to gastrulation (13–35hpf), 81–133hpf as competence to settle is developing, and 3–6hpi as polyp development is getting under way after settlement. Total numbers of genes up/downregulated during those periods were 28,254/20,115, 20,116/16,605, and 8198/10,742 respectively. For the purposes of this plot, the definition of genes likely to be involved in gene regulation was those with Gene Ontology annotations including the terms "regulation of gene expression," "transcription," "methylation," "chromatin," "transcriptional," "miRNA" or "mRNA". More detail on the methodology used is provided in the main text

support a 3-transition hypothesis of early coral development (Additional file 1: Fig. S1). Whilst such analyses are informative with respect to the major transitions in development, they are less useful for exploration of the expression patterns of subsets of genes in terms of structure or function according to Pfam or Gene Ontology (GO) IDs. To facilitate these latter kinds of analyses, a software tool based on the Shiny web framework was developed.

One powerful feature of the new software tool is that it allows the simultaneous visualisation of developmental gene expression patterns from a subset of genes defined by gene identifiers, Pfam domains or GO terms. These subsets can be selected for further analyses and comparison based on morphology, behaviour or gene expression patterns, such as those occurring during gastrulation and settlement.

Whilst early zygotic gene expression accompanied gastrulation, the major transition at 81–93hpf is likely to correspond to larval competence which is the preparation for settlement and metamorphosis. Both of these transitions have previously received considerable attention (e.g. [4, 13, 20]). Metamorphosis was underway by 3hpi and was followed by changes in the expression of large numbers of genes (Figs. 2, 3). This post-settlement change in the expression patterns of many coral genes has previously received only limited attention [25] and therefore merited closer examination. In what follows we have proceeded chronologically, with a particular focus on processes and classes of genes not discussed in previous studies.

Maternal transcripts and the earliest transcriptional events

As in most animals, early post-fertilisation development in corals consists of rapid cell division during which the maternal cytoplasm is serially subdivided (reviewed in [14]), and the transcripts required to facilitate these events are largely provided maternally. Extensive zygotic genome activation appears to be initiated leading into gastrulation (i.e. around 13 h post-fertilisation; Figs. 1, 2) corresponding to the "prawn chip" morphology.

Rapid rounds of cell division during early development require that replication occurs quickly, generating a need for core histone proteins in large amounts to form the H2A/H2B and H3/H4 dimers that constitute the nucleosomes responsible for packaging the DNA into chromatin. As in *Hydractinia* (*Klyxum*) *echinata* [39], histone mRNAs are amongst both the most abundant maternal transcripts and earliest expressed zygotic genes in *A. millepora* (Fig. 4A). Note, however, that the early zygotic (canonical) histone transcript profile is likely to be dominated by the replication-coupled types, i.e. those with expression tightly linked to the S-phase of cell division, as distinct from the replication-independent genes, with products expressed throughout the cell cycle.

Transcripts encoding the core histones H2B, H3 and H4 were particularly abundant in the *A. millepora* maternal mRNA complement (XP_029191967.2, XP_029210292.1 and XP_029195867.1 respectively in Fig. 4A), and the zygotic expression of these histone types began early at

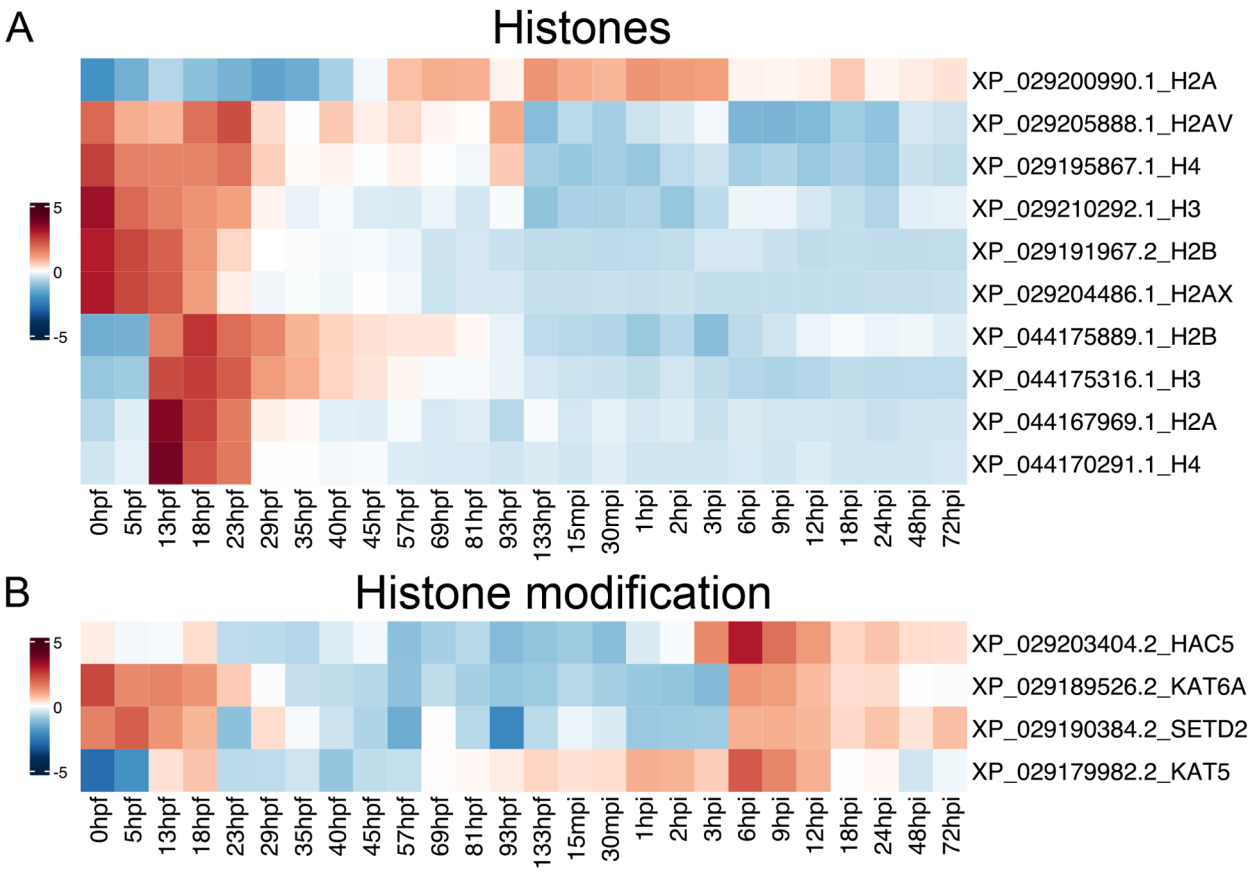

Fig. 4 Expression of histone genes and histone modifying enzymes during the early development of *Acropora millepora*. **A** Heatmap showing expression of selected histone genes during development. mRNAs encoding canonical histones H3, H4 and H2B are present at high levels in eggs (rows 3, 4 and 5 from the top), as are H2A.X and H2A.V (but not canonical H2A) messages. Zygotic expression of the four core canonical histones begins at the start of gastrulation (i.e. the 13hpf time point); note that the set of histone genes shown in the bottom four rows is likely to represent a replication-dependent subset that may be required at high levels only early in development. Consistent with this, the top row shows data for another H2A gene, expression of which begins later in development. **B** Heatmap showing expression of histone modifying enzymes during the early development of *A. millepora*. mRNAs encoding the histone acetyltransferase KAT6A and the histone H3K36 methylase SETD2 are maternal (rows 2 and 3, respectively). Two other histone acetyltransferases (HAC5 and KAT5; top and bottom rows) are most highly expressed at the 6hpi time point, reflecting their possible role in activating chromatin during the post-settlement transition. Note that a second wave of expression of both KAT6A and SETD2 also occurs at that time. All of the data points represented in the heat maps are the means of six individual measurements. Individual data points for each transcript can be viewed via the web app by un-ticking the "Average replicates" box

the onset of gastrulation with a peak at 13–18hpf for H3, H4 and H2B (XP_044175316.1, XP_044170291.1 and XP_044175889.1, respectively, in Fig. 4A).

Curiously, however, canonical H2A mRNA was not maternally provisioned at significant levels, instead, one of two H2A.X homologues (H2A.X2; XP_029204486.1) and, to a lesser extent, H2A.V (H2A.F/Z; XP_029205888.1) transcripts were maternal. Levels of mRNA encoding maternal H2A.X in the unfertilised eggs were very high but fell dramatically after 13hpf as zygotic expression of canonical H2A began (e.g. XP_044167969.1), and H2A.X transcripts were essentially absent by 29hpf (Fig. 4A).

Gastrulation is characterised by large-scale activation of the zygotic genome, requiring specific chromatin modifications. Consistent with this, high levels of mRNAs encoding homologues of the histone acetyltransferase (HAT) KAT6A (XP_029189526.2) and SETD2 (XP_029190384.2) were provided maternally (Fig. 4B). The latter is the only histone methyltransferase capable of generating the H3K36me3 modification essential for transcriptional activation [40]. Note that both of these genes were reactivated during the post-settlement transition discussed below.

The MZT occurring at gastrulation marks the first major developmental transition

To date, the process of gastrulation has been the most extensively studied aspect of developmental gene expression in both corals and in the sea anemone *Nematostella vectensis* [41]. In situ hybridisation analyses have shown that orthologs of several key developmental regulators from bilaterians are temporally and spatially expressed in *A. millepora* consistent with conservation of function. Examples of these include *snail* (Fig. 5) [18], *brachyury* [42, 43], *forkhead* [42] and *dpp/bmp4* [16] (Additional File 2: Fig.S2).

With the sole exception of *Pavona*, all complex corals examined to date go through a "prawn chip" stage of early development that corresponds to the early gastrula [44, 45]. At this stage, a homologue of *Drosophila* snail (XP_029185944.1) was expressed in the presumptive mesendoderm of *A. millepora* [18]. As snail-expressing cells are undergoing an epithelial-mesenchymal transition (EMT), one of several *A. millepora* genes related to *Drosophila* aristaless (XP_044163657.1XP_029193169.1) was expressed throughout the presumptive ectoderm (Fig. 5). Hence, these two genes effectively demarcate the two primary tissue layers of *A. millepora* during gastrulation.

The late planula transition corresponds to the acquisition of larval competence

During the period 81–93hpf, many genes show strong downregulation, but this is immediately followed by the upregulation of an even larger number of genes during the 93–133hpf time window (Fig. 3). These timepoints correspond to the acquisition of settlement competence and when *A. millepora* larvae are searching for cues that identify appropriate settlement sites (e.g. [5–8]) by swimming along the substratum to periodically sample it with the aboral end.

Settlement involves the aboral larval ectoderm making contact with substratum, which is likely coated with attractive and potentially hostile bacteria, and amongst the upregulated genes a number encode proteins with known or suspected antimicrobial properties. Amongst them are, for example, AmAMP1 [46] (XP_029188806.1), the MAC-Perforin protein apextrin [13, 47] (XP_044181104.1) and the quorum quenching enzyme AmNtNH1 [48] (XP_029207486.1). Figure 6 summarises developmental expression data for these three genes.

This study also provides the most direct evidence to date in support of Hadfield's hypothesis [49] that coral larvae are primed for settlement and metamorphosis via prior gene expression. Whilst several thousands of genes are up or downregulated during the onset of competency (81–133hpf), settlement and the initiation of metamorphosis largely happen without changes in gene expression (Fig. 3). With the caveat that datasets and technologies

(See figure on next page.)

Fig. 5 Heatmaps and in situ hybridisation provide complementary data for homologues of snail and homeobrain. During gastrulation, these genes have complementary morphological expression patterns, *Am-snail* marking the presumptive mesendoderm [18] and *Am-homeobrain* the presumptive ectoderm. **A** Diagrammatic vertical sections of embryos aged from early "prawn chip" to sphere. **B–D** Embryos aged from "prawn chip" to sphere (blastopore closure) viewed in three different ways. **B** Critical-point dried embryos viewed with scanning electron microscopy reveal the external morphology, **C** whole mount in situ hybridisation reveals the spatial expression of Am-snail. **D** Vertical sections of in situ preparations reveal the internal distribution of the expressing tissue in the developing mesendoderm. **E** Expression of Am-homeobrain in the developing ectoderm revealed using whole-mount in situ hybridisation. Note that the two genes are complementary in their expression. *C′*, *E′* Heatmap showing the relative expression of the two corresponding genes over the course of development. Parts of the figure were published in Hayward et al. [18] Development Genes & Evolution 214:257–260, Springer Nature. All of the data points represented in the heats map are the means of six individual measurements. Individual data points for each transcript can be viewed via the web app by un-ticking the "Average replicates" box

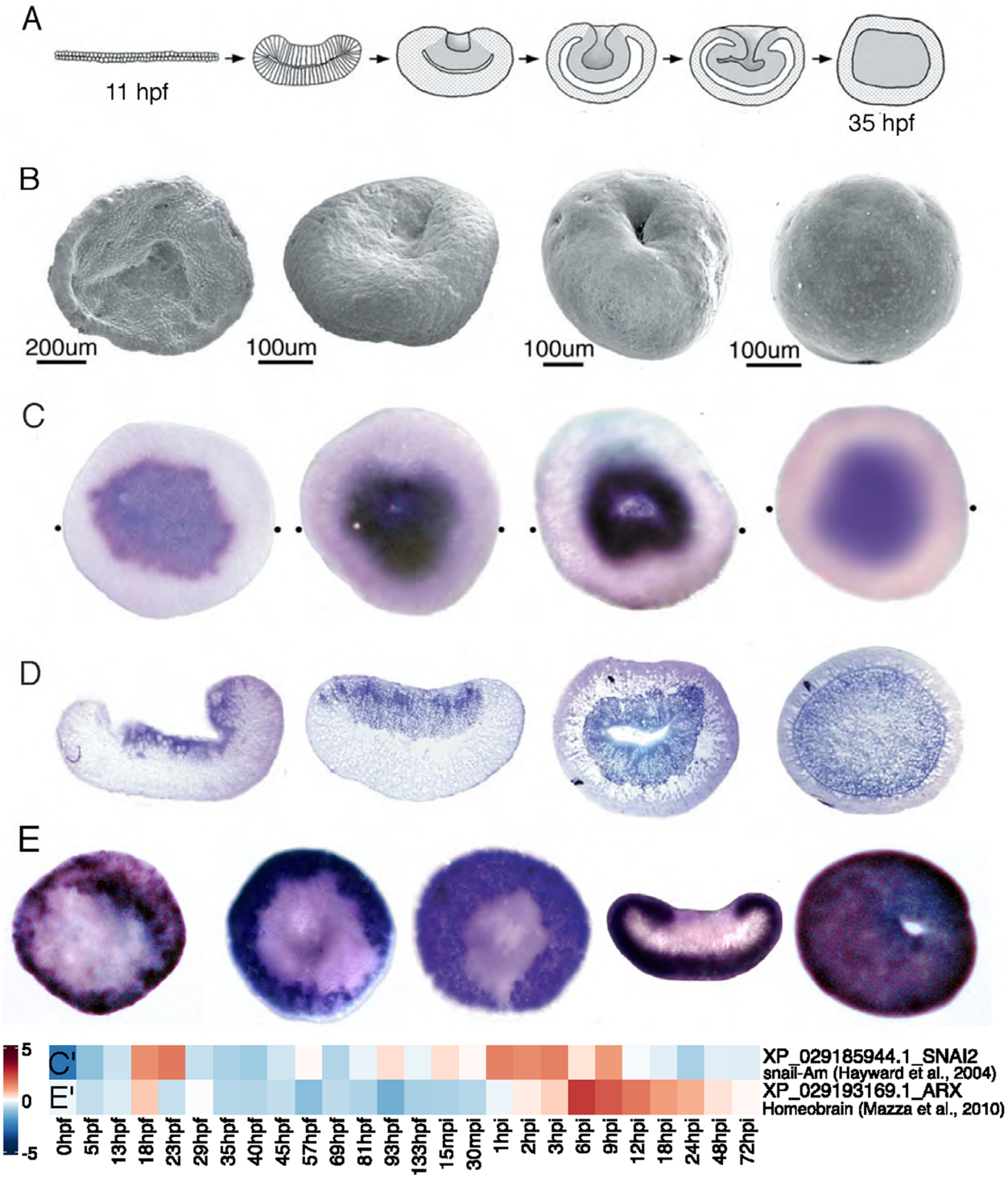

Fig. 5 (See legend on previous page.)

were much less sophisticated than those presently available, Grasso et al. [20] came to the same conclusion for *A millepora* based on microarrays, as did Strader et al. [4] indirectly by correlating expression data for competent larvae with data for settlement-induced larvae from Meyer et al. [22].

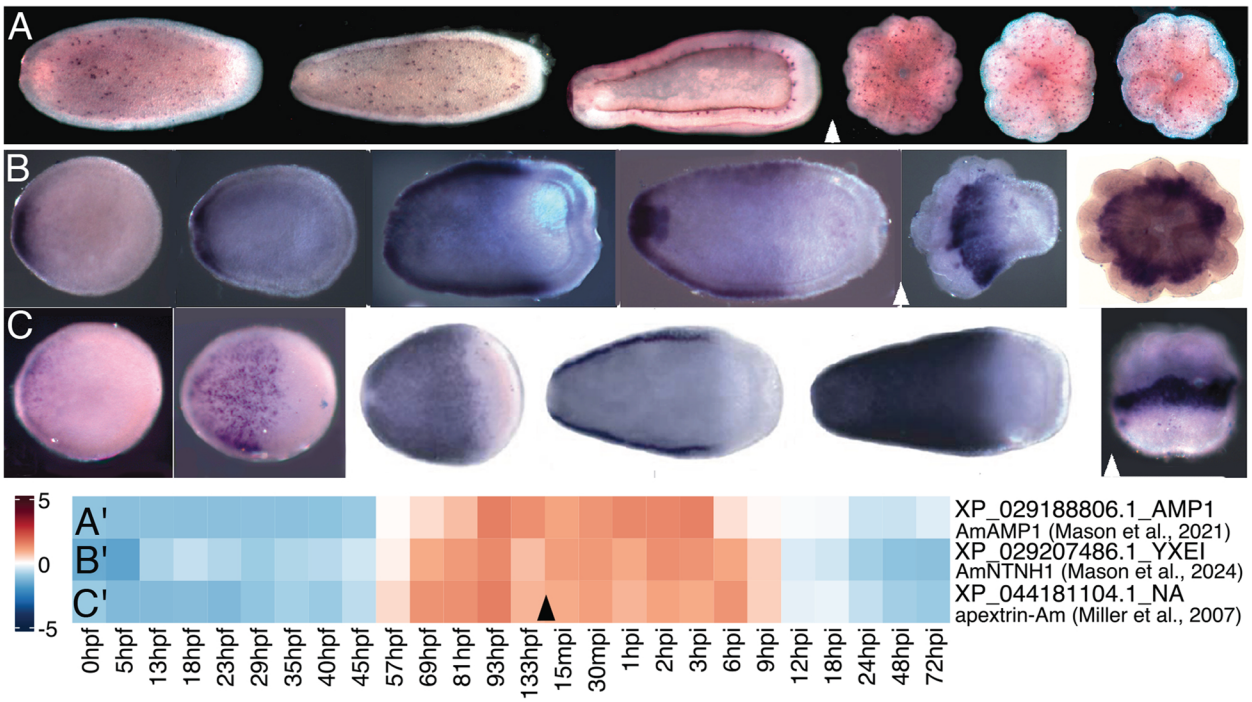

Fig. 6 Expression of known and suspected anti-bacterial activities during settlement and metamorphosis in *A. millepora*. The upper three rows show in situ hybridisation data for developmental stages leading into and immediately following settlement for **A** the anti-microbial protein AmAMP1 [46], **B** the quorum quenching activity AmNtNH1 [48] and **C** the MAC-Perforin protein Apextrin [13, 47]. *A′*, *B′* and *C′* are heatmaps showing the corresponding temporal expression levels of the three genes. The arrowheads indicate the time of settlement induction. All of the data points represented in the heat maps are the means of six individual measurements. Individual data points for each transcript can be viewed via the web app by un-ticking the "Average replicates" box

The post-settlement gene expression transition resembles an MZT in terms of scale and involvement of some specific components

The scale of the post-settlement transition between 3 and 6hpi resembles that typical of an MZT. In *A. millepora*, we estimate that approximately 20% of mRNAs undergo at least a two-fold change in expression level (i.e. are either up- or downregulated over the 3–6hpi time window). By comparison, in the zebrafish approximately 25% of maternal transcripts are cleared during the MZT [50] and the corresponding number for *Caenorhabditis* is around 33% [51]. Many of the mRNAs upregulated over the 3–6hpi time window in *A. millepora* coded for transcription factors or other regulatory proteins involved in chromatin modifications and mRNA processing.

Chromatin modification during early development and at the post-settlement transcriptional transition

Major changes in gene expression patterns also generally involve chromatin modification events, so histone modification and DNA methylation changes are to be expected. Homologues of a number of key chromatin modifiers are differentially expressed at the 3–6hpi transition.

In many animals, homologues of TET (ten-eleven translocation) are the primary agents responsible for demethylation of 5-methylcytosine residues (MeCpG) in DNA and are required for gene activation [52–54]. As well as a transient earlier (5hpf) window of expression leading into the early MZT, the *A. millepora TET* homologue (XP_029179484.2) was strongly upregulated at the 6hpi time point (Fig. 7A), suggesting a role in relieving repression by erasing pre-existing MeCpG marks.

DNA methylation is generally associated with repression of transcription, the enzymes associated with maintenance and de novo DNA methylation being the DNA methyltransferases DNMT1 and DNMT3, respectively.

In the case of *A. millepora*, mRNAs encoding the DNA methylases DNMT1 (XP_029197815.2) and DNMT3a (XP_029213858.1) were maternally provided, zygotic expression of DNMT1 being detected between 29hpf and 12hpi, despite having faded by 81hpf. Both DNMTs were upregulated 12 to 18hpi with expression of DNMT3a appearing to be stronger than that of DNMT1 (Fig. 7A).

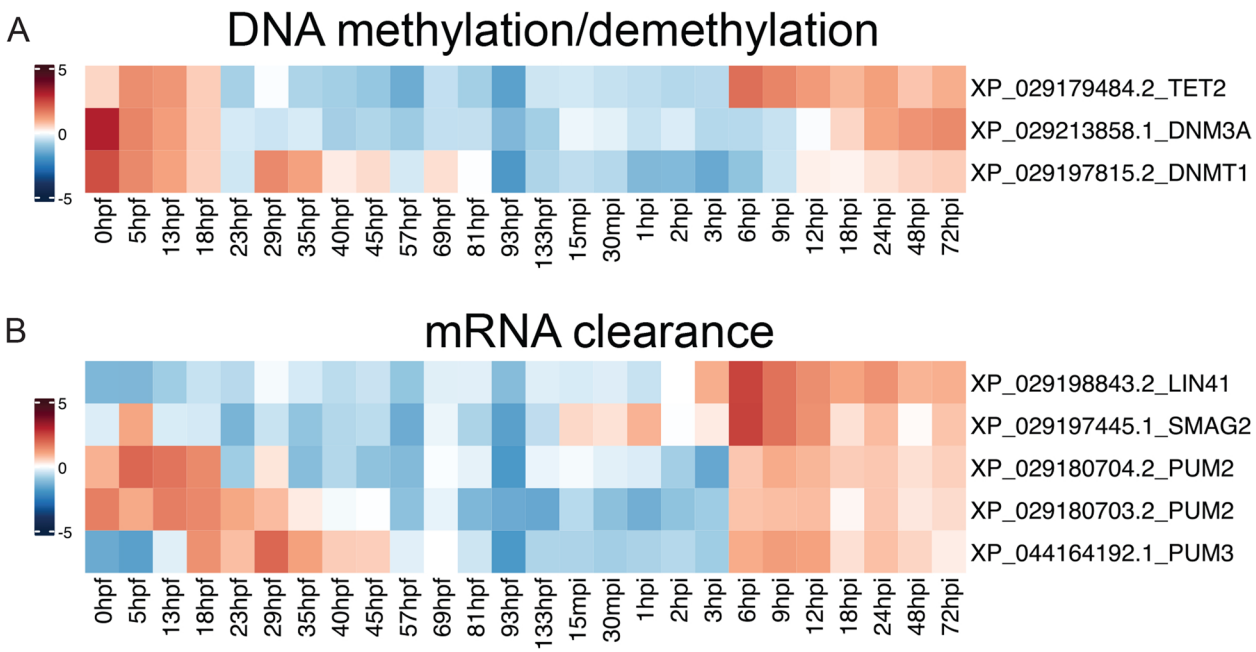

Fig. 7 Heatmaps for genes implicated in DNA methylation/demethylation and clearance of mRNAs and proteins. The upper panel **A** illustrates relative expression levels of the *A. millepora* homologues of ten-eleven-translocation (tet), the primary role of which is removal of CpG methylation marks, the de novo DNA methyltransferase, DNMT3, and the maintenance DNA methyltransferase, DNMT1. Although all three activities are expressed during gastrulation, TET is most highly expressed at the 6hpi time point. The lower panel **B** shows relative expression levels of *A. millepora* homologues of the conserved mRNA clearance activities, Smaug and Pumilio, and the TRIM-NHL ubiquitin ligase, TRIM71/LIN41. Smaug and TRIM71/LIN41 are most highly expressed at the 6hpi time point; three gene predictions annotated as Pumilio homologues (corresponding to at least two distinct gene products) were also upregulated at that time. All of the data points represented in the heat maps are the means of six individual measurements. Individual data points for each transcript can be viewed via the web app by un-ticking the "Average replicates" box

mRNA degradation during major transitions in development

One of the two major characteristics of MZTs is the elimination of a subset of maternally provided mRNAs (often a major proportion) to facilitate the transition to the zygotic developmental programme. The mRNA elimination process employs a range of mechanisms to destabilise or degrade transcripts, but some conserved players have been identified during major transitions, including homologues of the *Drosophila* genes Pumilio [55, 56] and Smaug [57]as well as the *Caenorhabditis* protein TRIM71/LIN41 [58].

Transcripts annotated as *Pumilio* (XP_029180703.2 and XP_029180704.2) were maternally provided but were essentially cleared after 29hpf, whereas a distinct Pumilio homologue (XP_044164192.1) was not represented in the maternal mRNA complement but was expressed from 18hpf (Fig. 7B). Each of these Pumilio homologues was upregulated over the 3–6hpi time window after earlier periods of activity.

Members of the Smaug/SAMD4 family of proteins are highly conserved (yeast to man) regulators of mRNA stability and transcriptional repressors that act in development by binding to specific RNA sequence motifs. Smaug proteins have been implicated in erasing maternal transcripts during the MZT in the early development of diverse animals [27, 57] implying that the Smaug homologue fulfills a similar function in the early development (around 4hpf) of the coral *Montipora capitata*. Although a minor peak of Smaug expression was observed at 5hpf, possibly corresponding to that reported in *Montipora capitata* [27], the *A. millepora* Smaug homologue (XP_029197445.1) was predominantly expressed at 15mpi–6hpi (peak) (Fig. 7B). A second transcript annotated as Smaug (XP_044163536.1) was mildly upregulated at 13–18hpf.

Members of the TRIM71/LIN41 family of E-3 ubiquitin ligases are highly conserved RNA-binding proteins [59] that facilitate major developmental transitions in *Caenorhabditis* [58]. At least one member of this gene family (XP_029198843.2/XP_029198844.2) is upregulated at the 3–6hpi time point during *A. millepora* development, suggesting that they may also be involved in protein clearance at the 3–6hpi transition.

Small RNA processing pathway components

Small RNAs (miRNAs, siRNAs and piRNAs) have important regulatory functions during the development of

many bilaterians [60] and this is likely to also be the case in *A. millepora* given that at least some components of the miRNA processing pathway are known to be differentially expressed during the development of *N. vectensis* [61]. In cnidarians, the biogenesis of miRNAs follows a plant-like pathway [62], but homologues of some of the enzymes in the animal miRNA processing system are also present and may also participate in miRNA synthesis. To address the possibility of miRNAs participating in gene regulation during early coral development, the expression of components of both the plant and animal processing pathways was investigated (Fig. 8).

Some of the small RNA processing pathway components were provided maternally, levels of transcripts annotated as Dicer-like (XP_029197160.2) and the HEN1 methyltransferase (HEN1MT; XP_029185006.2) being present at high levels. In cnidarians, HEN1 is responsible for methylation of the 3'-ends of both miRNAs and piRNAs, resulting in their stabilisation. The observed upregulation of HEN1 at 93hpf (Fig. 8) is consistent with a role in metamorphosis of *A. millepora* larvae, as in *N. vectensis* [63]. The *A. millepora* maternal mRNA repertoire also included an Argonaute homologue (XP_044181068.1) and a Piwi-like protein (XP_029187700.2/XP_029187701.2) (Fig. 8) that likely function together in transposon silencing during early development, as in *N. vectensis* [64, 65]. The high abundance of mRNA encoding a homologue of the Maelstrom protein (XP_044166539.1) also attests to the importance of the piRNA-mediated transposon silencing pathway [66, 67] during the earliest stages of coral development.

Although not maternal, other miRNA pathway components were expressed very early in development (Fig. 8). Transcripts annotated as DGCR8/Pasha (XP_029194207.2) and SRRT/Serrate (XP_044181962.1) were first detected as the early embryo was going into gastrulation at about 13hpf. For both of these genes, other transcripts carrying the same annotation were expressed during different stages of development. In the case of SRRT/Serrate, XP_044181962.1 is expressed in the early gastrula but maximally after the initiation of metamorphosis (6hpi). A second isoform/splice variant (XP_044181963.1) was most highly expressed very early in the settlement process (15mpi–2hpi)—i.e. prior to what Ishii et al. [25] referred to as the "point of no return". Similarly, the DGCR8/Pasha paralogs or splice variants XP_029194207.2 and XP_029194208.2 seem to have distinct expression profiles during development (data not shown). In addition to the maternal Piwi-like mRNA (XP_029187700.2/XP_029187701.2), a second (non-maternal) Piwi (XP_044168784.1/XP_044168785.1/XP_044168786.1) was expressed from the early gastrula

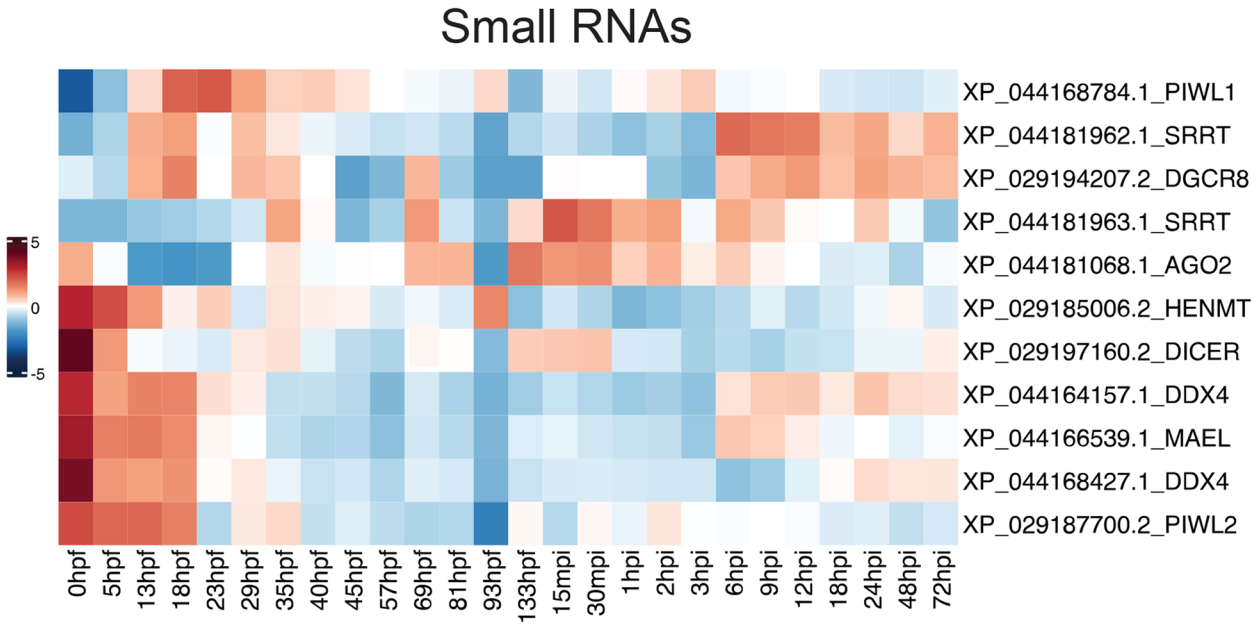

Fig. 8 Expression of genes involved in small RNA (miRNA and piRNA) processing during early development. mRNAs encoding HEN1 and Dicer homologues (rows 6 and 7) were present at high levels in eggs, as were those encoding homologues of Maelstrom, Vasa/DDX4.1 and.2, and Piwi2, which function primarily in piRNA-mediated transposon silencing. Other miRNA processing activities, including homologues of Serrate/SRRT and DGCR8/Pasha, were also expressed in embryos, larvae and during post settlement life, implying extensive involvement of miRNAs in regulating gene activities during early coral development. All of the data points represented in the heat maps are the means of six individual measurements. Individual data points for each transcript can be viewed via the web app by un-ticking the "Average replicates" box

stage, peaking in expression as the maternal type was fading.

Discussion

The study of early coral (*A. millepora)* development presented here was based on gene expression profiles obtained for 26 developmental stages spanning the period between unfertilised eggs and 3-day-old primary polyps. Analyses via the DEView app revealed three major transcriptomic transitions—the maternal-zygotic transition, the acquisition of competence by planulae (93–133hpf) and a post-settlement transition (3–6hpi) that has not previously received significant attention. This latter novel transition in gene expression resembled an MZT in terms of scale and the involvement of some key genes. In addition to regulatory genes involved in key chromatin modification activities and RNA processing, we focussed here on genes likely to have protective roles, specifically those potentially involved in anti-microbial activity and transposon silencing.

We deliberately chose to adopt a non-statistical approach in deciding what questions to investigate in detail and how to present the results. Whilst this may seem counter-intuitive, we argue that basing conclusions on changes in the expression of whole suites of genes—as has previously often been the case—may result in swamping "signals" from critical regulatory genes in the background "noise" generated by many other genes. For example, trimethylation of H3K36 is a key event in gene activation; SETD2, the only protein capable of that transformation, is one of 82 hits found when searching our dataset using the term "Histone-lysine N-methyltransferase". A caveat to our approach, however, is that focussing on specific key genes brings with it the possibility of missing other important changes.

In many animals, mRNAs encoding canonical histones (including H2A), as well as the corresponding proteins, are provided maternally at sufficient levels to support the earliest cell division events. Cnidarians lack protamines, instead packaging sperm using histones that are predominantly specialised H1 and H2B variants [68, 69]. To our knowledge, the finding that in *A. millepora*, an mRNA encoding one H2A.X variant (H2A.XII) replaced that for canonical H2A in the eggs is novel. H2A.X is a histone variant with a best-defined role in DNA repair [70, 71]. It is closely related to canonical H2A but distinguished from it by the presence of a characteristic C-terminal sequence extension that includes a serine residue subject to phosphorylation, thus generating the gammaH2A.X form which is required for binding at double-stranded DNA breaks [72]. The enzymes responsible for this phosphorylation of H2A.X are Phosphoinositide-3-Kinase-related protein kinases (PIKKs), and at least one PIKK-related protein kinase (XP_029200091.2) is provided maternally in *A. millepora*, though it is unclear whether H2A.X is a substrate for this activity.

In *A. millepora* H2A.X2 mRNA may be maternally provided at high levels to facilitate maintenance of DNA integrity through the earliest developmental stages. This may also be the case in cnidarians more generally, as an H2A.X variant is expressed in female germ cells in *Hydractinia (Klyxum) echinata* [69]. Chille et al. [27] noted high representation of GO terms associated with DNA repair in the maternal mRNA complement of *Montipora capitata*. There is a second H2A.X-like gene (H2A.X1; XP_029200990.1—annotated as H2A-like) in *A. millepora* that is minimally expressed during early development.

Comparisons with published studies of coral development

Development has been studied primarily in members of the three coral genera: *Acropora, Montipora* and *Porites*. Whilst these are all members of the "superfamily" Complexa, and the first two belong to the same coral family (Acroporidae), one important difference is that both *Montipora* spp. and *Porites* spp. maternally transmit Symbiodiniaceae whereas *Acropora* spp. acquire their symbionts from the environment during early life. Comparisons between the work presented here and previously published papers in this field (Table 1) are complicated due to the diversity of species studied, differing temperatures during development, differing sampling points and differing inducers used to trigger settlement and metamorphosis. So, whilst the major morphological stages can be compared, and the progression of events is the same, detailed interspecific or inter-study comparisons are difficult.

Our most interesting observation was the extent and nature of the post-settlement transcriptional transition observed at 3–6hpi. This major change in gene expression is more apparent than in previous studies which either did not include post-settlement stages [4, 27] or sampled sparsely pre-settlement [30] or after settlement induction [22, 25] (Table 1). Chille et al. [27] focussed on the MZT and therefore studied gene expression changes during development of *Montipora capitata* from unfertilised egg to planula, in addition to adults. Some of their MZT results are consistent with those presented here for *A. millepora*, for example the expression of Smaug (although in our study, the major peak of expression occurred during the post-settlement transition; Fig. 7B) and Brachyury (Additional File 2; Fig. S2) in the "prawn chip" and early gastrula. Using GO-term data, Huffmyer et al. [30] recognised three distinct (but overlapping) phases of gene expression during the early development of *M. capitata*. The 3–6hpi gene expression

transition observed here may correspond to what Ishii et al. [25] refer to as "the point of no return" (PNR), a point in post-settlement development after which reversibility by aborting settlement and returning to the motile phase is lost. Whilst the Ishii et al. [25] paper focussed on gene expression changes between three time points during metamorphosis in *A. tenuis*, comparison between their results and those presented here is complicated by the differing triggers used to drive the process. For *Acropora* spp., external exposure of competent larvae to the *Hydra* GLWamide (Hym-248), directly triggers metamorphosis, essentially overriding the need for external settlement cues [20, 73, 74]. Whilst Ishii et al. [25] induced metamorphosis using Hym-248, the study described here triggered settlement by addition of CCA extract, which induces searching behaviour rather than directly driving metamorphosis [20]. Hence, it is not possible to directly compare developmental timing between these two studies. The 1hpi and 6hpi time points in the Ishii paper are likely to correspond to later time points in the present study, as the duration of the settlement period must be several hours longer when using CCA extract compared to Hym-248. The PNR inferred by Ishii as occurring at 4hpi may correspond to the 3–6 h transition identified in the present work but note that rates of development can be strongly influenced by temperature. The differences in gene expression between untreated (0 h) and 1 h after induction described in the Ishii et al. [25] paper are therefore likely to encompass a number of distinct time points in our study, so subtle transcriptional changes occurring during the searching and very early settlement phases were presumably not noted by Ishii et al. [25].

The post-settlement transition—a cnidarian equivalent of the *Caenorhabditis* "juvenile to adult" transition?

The transcriptomic transition from larvae to recruits at 3–6hpi in *A. millepora* has several parallels to maternal-zygotic transitions [75] regarding the removal of earlier transcripts and genome activation appropriate for stages following the transition. A precedent for such a later transition is provided by *Caenorhabditis elegans*, where it is recognised as the juvenile to adult transition [58].

Above, the involvement of homologues of both *Drosophila* Smaug and Pumilio in the mRNA clearance processes during MZT and the juvenile to adult transition at 3–6hpi were highlighted. In addition, two transcripts corresponding to the same sequence (XP_029198843.2 and XP_029198844.2) which is annotated as a member of the TRIM71/LIN41 family of RNA-binding proteins, were upregulated during the 3–6hpi transition. Other members of this protein family have important roles in the regulation of both oocyte to embryo [58] and juvenile to adult [76] developmental transitions in *Caenorhabditis*. As in *Caenorhabditis* [58], this *A. millepora* TRIM71/LIN41-related protein is likely to be involved in regulatory changes at the 3–6hpi transition, and on this basis deserves further exploration.

In addition, peaks in the expression of the DNA demethylase TET (Fig. 7A) and of SETD2 (XP_029190384.2) as well as homologues of the histone acetyltransferases HAC5 (XP_029203404.2), KAT5 (XP_029179982.2) and KAT6A (XP_029189526.2) (Fig. 4B) around 3–6hpi imply that important chromatin modification events occur at that time. Presumably, the corresponding proteins function in facilitating transcription of genes required for early polyp development. Transcription factors (TF) strongly upregulated at the 3–6hpi time point include genes annotated as homologues of FoxB1 (XP029196672.1) and FoxO (XP_029208531.2), Aristaless (XP_029193170.1), Rax (XP_029193171.1), Meis2 (XP_029187327.1) and Otx (XP_029190339.1), whilst homologues of Emx (XP_029211983.2), Pitx2 (XP_029179676.1) and Brn3C (XP_029213135.1) were simultaneously downregulated.

Limitations: heatmaps are useful but tell only part of the story

One feature of the heatmaps produced by DEView is that the upper limit of expression (i.e. the darkest red colour) is determined by the most-expressed gene included in that map, so important changes in gene expression may not be as apparent as if the gene was plotted against itself. A further caveat in making inferences from heatmaps across developmental stages, and more generally from whole-larvae overall expression levels, is that important subtle changes may be missed. Particularly with transcription factors or other regulatory molecules, low overall levels of expression may have major effects, especially when restricted to subsets of cells. Consequently, interpreting developmental gene expression requires not only temporal data, but also spatial information from the application of in situ hybridisation or other techniques. This is clearly illustrated in Additional File 2: Fig.S2, which provides expression data for genes implicated in conserved functions during gastrulation.

Whilst in situ hybridisation data show expression of these four genes in smaller subsets of cells across all developmental stages between gastrulation and metamorphosed recruit, the heatmaps show that the expression maxima occur post-settlement rather than at gastrulation around 13–18hpf. Only a weaker peak in expression of Brachyury at 13hpf corresponds to the early gastrulation window of expression visualised via in situ hybridisation [42]. Consequently, visualisations of spatial expression via in situ hybridisation are required to study the function of selected genes. For example, whilst

gene expression data presented in the heatmap suggested functions post-settlement, ISH visualisations revealed that temporal expression of an *A. millepora* arx-related gene (XP_044163657.1/XP_029193169.1) during gastrulation closely complements that of snail (Fig. 5). This *A. millepora* sequence is referred to here as homeobrain, based on its orthology with XP_048583705.1 from *N. vectensis* [77]. Snail and homeobrain respectively demarcate the early mesendoderm and presumptive ectoderm during gastrulation (Fig. 5), but both are also expressed at higher levels after settlement-induction where snail expression reaches its expression peak earlier than in the case of homeobrain. Assuming these two genes fulfill similar functions during gastrulation and post-settlement, this suggests that a cell migration such as in an epithelial-mesenchymal transition occurs during the initiation of metamorphosis.

Expression of the small RNA processing machinery during early development

Despite deep evolutionary divergence between the sea anemones (Actiniaria) and the coral/corallimorpharian lineage, many of the molecular processes underlying early development in *A. millepora* closely parallel those described in *N. vectensis* [41, 42], and this appears to extend to the machinery for processing small RNAs (miRNAs and piRNAs). However, some differences were observed in the timing of expression of several of the genes implicated in small RNA processing. Whilst mRNAs for Vasa1, Maelstrom and Piwi are provided maternally in *A. millepora* and *N. vectensis*, Vasa2 (aka Vasa-like or DDX4) is also maternal in the coral whereas the corresponding mRNA was not detected until around gastrulation in *N. vectensis* [61]. Whether Dicer/DCL is maternal is unclear in the case of *N. vectensis*, whereas mRNA of the *A. millepora* homologue of *N. vectensis* Dicer 2 (AGW15596.1), encoding XP_029197160.2, is abundant in *A. millepora* eggs. In summary, the preliminary data presented here indicate that all or most of the small RNA processing machinery is either maternal or expressed very early in *A. millepora* development. It is therefore likely that, in addition to roles for some of these components in transposon silencing, miRNAs have important regulatory roles in the early development of *Acropora* spp.

Heatmaps enable identification of candidate genes for key roles in early development

A major strength of the DEView app is that it provides a means of scanning classes of genes individually or collectively for their expression patterns across early coral development, allowing identification of candidates for roles in specific processes, including settlement induction and the initiation of calcification. Whilst significant progress has recently been made, we have as yet a relatively limited understanding of the nature and recognition of settlement cues [8, 14, 78, 79]. The larvae of many corals select appropriate settlement sites by detection of small molecules that either favour or discourage settlement [5, 7, 80–84]. Most likely the outcome reflects a combination of molecules acting as ligands for specific receptors that are expressed in competent larvae and downregulated after settlement and metamorphosis. Receptors that potentially could be involved in settlement cue reception and downstream signalling pathways, respectively, are G-Protein coupled receptors (GPCRs) and nuclear receptors. With the help of the DEView app, search terms such as "G-protein coupled receptor" or specific Pfam domains can be used as filters to search the developmental transcriptome to identify genes that were upregulated at competency (i.e. 93hpf) consistent with their potential involvement in settlement cue perception. Searching the *A. millepora* data using the terms PF00104 Ligand-binding domain of nuclear hormone receptor and PF00105 Zinc finger, C4 type (two domains) yielded 21 hits corresponding to 14 loci (Additional File 3: Fig. S3). Nuclear receptors play key roles in metamorphosis in both insects and some vertebrates, potentially acting in the internal transmission of metamorphosis signals rather than their external reception. Of the 14, seven were upregulated at 133hpf and all of these mRNAs appear to be cleared at the 3–6hpi transition, so they could have roles in the cue recognition pathway and/or metamorphosis.

Conclusions

The *A. millepora* developmental transcriptome data, together with the DEView app, have provided novel insights into early coral development and allowed identification of candidate genes for key roles. We hope that the availability of this app via the web will lead to more extensive exploration of the data and ultimately facilitate much better understanding of the molecular processes underlying the development of the coral body plan. The approach developed for this study can be built on and modified to study developmental gene expression changes in other species with well-developed transcriptomic datasets.

Methods

Sample collection

Colonies of *Acropora millepora* were collected at Orpheus Island, Queensland, Australia, (18.6141° S, 146.4892° E) under GBRMPA permit G13/36196.1 shortly before they spawned at approximately 9 pm on 21 November 2013. The samples sequenced were the result of reciprocal crosses between two colonies and were

raised in three separate flow-through tanks to control for tank effects.

Material was collected from 26 different time points of which 14 were sampled before and 12 after settlement induction. Pre-settlement, samples were collected from unfertilised eggs, at 5 h post-fertilisation (hpf; 16–64 cell stages), 13hpf ("prawn chip"), 18hpf, 23hpf, 29hpf, 35hpf, 40hpf (sphere, some swimming), 45hpf (spheres, all swimming), 57hpf, 69hpf, 81hpf (planulae prior to the searching phase), 93hpf (searching planulae) and at 133hpf. At these stages, approx. 500 embryos per replicate ($n=3$) and cross ($n=2$) were immersed in 2 mL ethanol (100%). This caused them to sink to the tube bottom, so that the overlying liquid could be removed before tubes were snap-frozen in liquid nitrogen.

To assess settlement competency, between 69 and 93hpf, aliquots of planulae were exposed (independently) to either ethanolic extracts of the crustose coralline alga (CCA) *Porolithon onkodes* (kindly provided by Mikhail V. Matz; prepared as described in [85]) or the neuropeptide Hym-248, both of which are known to induce settlement of *A. millepora* planulae. At the 93 hpf stage 100% of planulae rapidly responded to the CCA extract by undergoing settlement followed by metamorphosis, hence the settlement-induced stages used for RNAseq were derived from planulae exposed to this inducer. Post-settlement samples were collected by stocking 144 petri dishes (2 replicates × 3 larval tanks × 2 crosses × 12 time points) with respectively 100 larvae at the age of 133 h. Settlement was induced with ethanolic CCA extract in all petri dishes at the same time. At the respective sampling times of 15 min after induction (mpi), 30mpi, 1, 2, 3, 6, 9, 12, 18, 24, 48 and 72 h post induction (hpi), unattached larvae were transferred into tubes, and attached settlers were snap-frozen on petri dishes using liquid nitrogen after excess seawater was decanted. Sample tubes and petri dishes were taken to James Cook University, (Townsville, Australia) in dry-ice, and stored at − 80 C until further processing.

RNA preparation and sequencing

Frozen samples in the plates were submerged in RNAlater-ICE and allowed to come to − 20 °C. Once thawed, RNAlater-ICE was removed and replaced by 2 ml of *mir*Vana™ homogenisation buffer. Polyps were gently scraped off the plate with a sterilised scalpel in the homogenisation buffer and transferred into a 2-ml tube for immediate processing.

For both pre- and post-settlement samples, total RNA was extracted using the *mir*Vana™ miRNA Isolation Kit (Invitrogen AM1560) according to the manufacturer's instructions. RNA quantity and quality were assessed using a NanoDrop ND-1000 spectrometer and denaturing gel electrophoresis using standard methods [86] before being shipped on dry-ice to AGRF in Brisbane for (100 bp paired-end) sequencing on a Hi-Seq 2500 machine. Sequencing data have been deposited at NCBI under bioproject PRJNA1332262.

Processing of sequence data

RNA sequencing data for all samples was first checked for quality and contamination using a Nextflow [87] pipeline https://github.com/marine-omics/moqc. This pipeline includes fastqc (v0.11.5; https://www.bioinformatics.babraham.ac.uk/projects/fastqc/) to check raw read quality, and read-level taxonomic classification via KrakenUniq (v1.0.2) [88] to determine the dominant symbiont genus and check for bacterial or eukaryotic contaminants. All samples were dominated by reads attributable to the coral host but also contained a small fraction (0.5–2%) from Symbiodiniaceae, of which *Durusdinium* was the dominant genus. No samples were flagged as having low-quality base calls, excessive adapter contamination or high levels of potential contaminants (e.g. bacteria). After confirming the overall quality of read data for all samples, reads were trimmed using fastp [89] to remove adapters and low-quality sequences.

Bioinformatic analyses of processed data

Trimmed reads were aligned to a combined reference database consisting of all *A. millepora* transcripts predicted from gene models along with the transcriptome of an unnamed *Durusdinium* species [90]. Alignment was performed using Bowtie2 (v2.5.0) [91] as part of RSEM (v1.3.3) [92] and used to produce transcript level counts for each sample. All of these steps were run using a Nextflow pipeline https://github.com/marine-omics/morp. Transcript counts produced by RSEM were imported into R and processed using the variance stabilising transform function in DESeq2 (v1.38.3) [93] to produce values on a log2 scale for visualisation.

Functional annotations for *A. millepora* transcripts were obtained using a nextflow pipeline (https://github.com/marine-omics/moat) that is primarily based around identifying homologous proteins in Swissprot (downloaded December 2022) via blastp and blastx (NCBI Blast + v 2.13.0). In this process, any protein with an evalue less than 1e − 5 is considered a hit and the best hit is used to lookup Gene Ontology ID's and a protein name from the Swissprot database. In addition, transcripts were annotated with conserved domains, gene family membership and an alternative Gene Ontology ID inferred using Interproscan (v5.59–91.0) [94].

Principal component analysis (PCA) was conducted using the prcomp function of the stats package in R with vst normalised counts.

Complete details of all data processing steps including scripts used for quality control, read mapping, statistical analysis of counts and functional annotation of genes are provided online at https://github.com/iracooke/amil2_dev with the version used for this manuscript archived via Zenodo (https://doi.org/10.5281/zenodo.17230817).

Weighted gene co-expression network analysis (WGCNA) was conducted with normalised data that were filtered for genes with excessive number of missing values or zero-variance using the goodSamplesGenes function of the WGCNA package [38]. The samples were clustered using the function hclust of the stats package [95] to detect outliers. One sample collected 3 hpi was removed from the analysis. To determine groups of genes (modules) with correlated developmental gene expression profiles, a weighted gene co-expression network was constructed blockwise using the function blockwiseModules with a maximum block size of 18,000 genes, a minimal module size of 18 and a mergeCutHeight set to 0.25. A signed, scale-free topological overlap matrix for each block was created by choosing a soft threshold power of 12 and a biweight midcorrelation.

Web browser development

To facilitate reuse and rapid exploration of the *A. millepora* developmental transcriptome, we created an interactive web application using the Shiny framework [96]. This application is hosted on servers provided by the Australian Research Data Commons Nectar Research Cloud to ensure that it is scalable and highly available for long-term use. Users can access the web application directly at https://amil-deview.mmb.group/ or obtain its source code and the underlying data from our github repository (https://github.com/iracooke/amil2_dev.). The application is designed to facilitate access to developmental expression profiles for individual genes or groups of genes. Users can define genes of interest in two ways; by either conducting a BLAST search of a sequence or by directly searching for genes with metadata matching a set of gene identifiers, Pfam domains, GO term IDs or text as part of the protein name. Once a list of genes has been identified, the corresponding normalised gene expression data are rapidly retrieved from an sqlite relational database and used to generate an interactive display. When the number of genes is small (default < 10) each gene is displayed using a separate line plot generated by the R package ggplot2 [97] so that detailed changes in the expression of each gene can be carefully inspected. For larger numbers of genes (default > = 10), we assume that the user is more interested in broad patterns amongst genes and the display changes to an interactive heatmap generated with the R package InteractiveComplexHeatmap [98]. In both cases, a list of genes with annotation information is also displayed and users can select rows in this table to adjust which genes are displayed in the main display. Comprehensive data and code exporting functions are also provided so that users can easily export both data and R code to reproduce the plots seen in the app to allow further customisation by the user.

Fixation and in situ hybridisation

Preparation of embryos and larvae for in situ hybridisation is described by Hayward et al. [99] and production of antisense digoxygenin-labelled probes from plasmid templates by Kucharski et al. [100]. In brief, specimens were fixed for 10–20 min in 3.7% formaldehyde in filtered sea water buffered to pH 8.0 with HEPES buffer. They were then washed repeatedly in filtered seawater, dehydrated through a graded methanol series and stored in absolute methanol at −20 °C. Before hybridisation, they were gradually rehydrated and returned to PBS at room temperature. They were then delipified using the RIPA solution of Rosen and Beddington (1993) [101] or sequentially by RIPA and Xylene. After washing in PBT (1X PBS; 0.1% Tween20), the specimens were placed in hybridisation solution (details in [100]). Digoxygenin (DIG)-labelled probes were produced by run-off transcription and corresponded to the entire length of the cDNA. To increase probe penetration, probe length was reduced by hydrolysis in 0.1 M sodium carbonate [100]. Probe was added to specimens in hybridisation buffer at a concentration of 0.1–1 µg/ml and hybridisation was carried out at 55 °C for 24 h. Following thorough washing in 50% formamide, 4×SSC, 0.1% Tween 20 at 55 °C, specimens were returned to PBT. The DIG signal was detected with an alkaline phosphatase conjugated anti-DIG antibody (Boehringer Mannheim). Specimens were cleared through a glycerol series, mounted in 90% glycerol, and viewed and photographed on a Wild M400 microscope.

Abbreviations

CCA	Crustose coralline algae
DIG	Digoxygenin
dpf	Days post-fertilisation
EMT	Epithelial-mesenchymal transition
EST	Expressed sequence tag
GBRMPA	Great Barrier Reef Marine Park Authority
GO	Gene Ontology
GPCR	G-Protein Coupled Receptor
hpf	Hours post-fertilisation
hpi	Hours post-induction
miRNA	MicroRNA
mpi	Minutes post-induction
MZT	Maternal/zygotic transition
PBT	1X PBS; 0.1% Tween20
PCA	Principal component analysis
Pfam	Protein family
piRNA	Piwi-interacting RNA

PNR	Point of no return
RNAseq	RNA sequencing
RSEM	Relative standard error of the mean
SEM	Scanning electron microscopy
siRNA	Small interfering RNA
SSC	Saline sodium citrate
TET	Ten-eleven translocation
TF	Transcription factor
WGCNA	Weighted gene co-expression network

Supplementary Information

The online version contains supplementary material available at https://doi.org/10.1186/s12915-026-02507-9.

Additional file 1: Fig. S1. Weighted gene co-expression network analysis (WGCNA) clustering of the developmental gene expression data. WGCNA clustered the developmental gene expression data into 39 modules based on correlated expression patterns. The number of genes in each module ranges from 18 (plum module) to 5851 (turquoise module) and the grey module contains all genes that did not fit into any other module. The WGCNA heatmap indicated that there is a major change in gene expression between 3 and 6 hours post induction (hpi) and also showed that settlement induction at the age of 133 hours post fertilisation (hpf) did not trigger an immediate strong change in gene expression 15 minutes post induction (mpi).

Additional file 2: Fig. S2. Spatial and temporal expression data for genes previously characterised in the context of gastrulation. In situ data for the *A. millepora* homologs of several genes imply conservation of function with Bilateria during gastrulation. (A) BMP2/4 (BMP2B), (B) forkhead (FOXA2), (C) goosecoid (GSC) and (D) brachyury (TBXT). However, heatmaps show that, for most of these genes, rather than at gastrulation (around 13 – 18 hpf) the expression maxima occur post-settlement. Only one of the genes previously characterised in the context of gastrulation (snail) has a major peak of expression at the late "prawn chip" (gastrula) stage (Figure 5) – which is consistent with in situ data [15] suggesting expression throughout the presumptive mesendoderm. All of the data points represented in the heat maps are the means of six individual measurements. Individual data points for each transcript can be viewed via the web app by un-ticking the "Average replicates" box.

Additional file 3: Fig. S3. Differential expression of genes encoding nuclear receptors during coral development. Searching the *A. millepora* data using the terms PF00104 Ligand-binding domain of nuclear hormone receptor and PF00105 Zinc finger, C4 type (two domains) yielded hits corresponding to 14 loci. Two of these loci code for predicted protein isoforms with distinct expression profiles (XP_029208454.1 and XP_029208455.1 are protein isoforms from the locus LOC114972094; XP_044184859.1 and XP_044184860.1 are isoforms from the locus LOC114969161). Consistent with possible roles in cue recognition and/ or metamorphosis, seven of the 14 genes were upregulated at 133hpf. All of these mRNAs were cleared at the 3-6hpi transition. All of the data points represented in the heat maps are the means of six individual measurements. Individual data points for each transcript can be viewed via the web app by un-ticking the "Average replicates" box.

Acknowledgements
The authors gratefully acknowledge the support of the Australian Research-Council under Discovery Grants DP170104734 and DP240102310, Super-Science Grant (round 2) FS110200046 and Centres of Excellence Grant CE14100020. We also thank Gergely Torda and the staff of the Orpheus Island Research Centre for fieldwork assistance. Some of the in situ images presented here were produced by Lauretta Grasso and Nikki Hislop.

Authors' contributions
Designed research: AM, DH, BL, EB, DM Carried out field work: AM, BL, EB Laboratory work: AM, BL Performed bioinformatic analyses: SF, AM, DH, IC Contributed new analytical tools: IC Analysed the data: AM, RB, MG, DH, DM Wrote the paper: DH, RB, EB, IC, DM (lead) All authors read and approved the final manuscript.

Funding
The authors gratefully acknowledge the support of the Australian Research. Council under Discovery Grants DP170104734 and DP240102310, Super-Science Grant (round 2) FS110200046 and Centres of Excellence Grant CE14100020.

Data availability
All data generated or analysed during this study are included in this published article, its supplementary information files and publicly available repositories. The dataset supporting the conclusions of this article is available in the NCBI BioProject repository [https://www.ncbi.nlm.nih.gov/bioproject/?term=PRJNA1332262].
To facilitate use and rapid exploration of the developmental transcriptome we created an interactive web application that is hosted on servers provided by the Australian Research Data Commons Nectar Research Cloud to ensure that it is scalable and will be accessible over the long-term. Users can access the web application directly at https://amil-deview.mmb.group or obtain its source code and the underlying data from our github repository (https://github.com/iracooke/amil2/_dev).

Declarations

Ethics approval and consent to participate
Our work does not require ethics approval, but all work involving the biota of the Great Barrier Reef requires approval by The Great Barrier Reef Marine Park Authority (GBRMPA) which rigorously assesses research plans before issuing appropriate permits and carries out routine surveillance. The work described here was conducted under GBRMPA permit G13/36196.1.

Consent for publication
The authors have all been consulted on draft and final versions of the manuscript and have consented to publication. All analyses have been subject to scrutiny by other authors and can be confirmed using the web-based tool that we have released (see below).

Competing interests
The authors declare no competing interests.

Author details
[1]ARC Centre of Excellence for Coral Reef Studies, James Cook University, Townsville, QLD 4811, Australia. [2]Molecular Genetics Unit, James Cook University, Townsville, QLD 4811, Australia. [3]Research School of Biology, Australian National University, Acton, ACT 2601, Australia. [4]Laboratoire d'excellence CORAIL, Centre de Recherches Insulaires Et Observatoire de L'Environnement (CRIOBE), Moorea, Papeete, B.P. 1013, French Polynesia. [5]Department of Marine Biology and Aquaculture, James Cook University, Townsville, QLD 4811, Australia.

Received: 17 June 2025 Accepted: 7 January 2026
Published online: 29 January 2026

References

1. Harrison PL, Babcock RC, Bull GD, Oliver JK, Wallace CC, Willis BL. Mass spawning in tropical reef corals. Science. 1984;223:1186–9. https://doi.org/10.1126/science.223.4641.1186.
2. Baird AH, Guest JR, Willis BL. Systematic and biogeographical patterns in the reproductive biology of scleractinian corals. Annu Rev Ecol Evol Syst. 2009;40:551–71. https://doi.org/10.1146/annurev.ecolsys.110308.120220.
3. Harrison PL. Sexual reproduction of scleractinian corals. In: Dubinsky Z, Stambler N, editors. Coral Reefs: An Ecosystem in Transition. Dordrecht: Springer Netherlands; 2011. p. 59–85. https://doi.org/10.1007/978-94-007-0114-4_6.
4. Strader ME, Aglyamova GV, Matz MV. Molecular characterization of larval development from fertilization to metamorphosis in a reef-building coral. BMC Genomics. 2018;19:1–17. https://doi.org/10.1186/s12864-017-4392-0.

5. Tebben J, Motti CA, Siboni N, Tapiolas DM, Negri AP, Schupp PJ, et al. Chemical mediation of coral larval settlement by crustose coralline algae. Sci Rep. 2015. https://doi.org/10.1038/srep10803.
6. Siboni N, Abrego D, Puill-Stephan E, King WL, Bourne DG, Raina J-B, et al. Crustose coralline algae that promote coral larval settlement harbor distinct surface bacterial communities. Coral Reefs. 2020;39:1703–13. https://doi.org/10.1007/s00338-020-01997-5.
7. Quinlan ZA, Bennett M-J, Arts MGI, Levenstein M, Flores D, Tholen HM, et al. Coral larval settlement induction using tissue-associated and exuded coralline algae metabolites and the identification of putative chemical cues. Proc Biol Sci. 2023;290:20231476. https://doi.org/10.1098/rspb.2023.1476.
8. Turnlund AC, O'Brien PA, Rix L, Webster N, Lurgi M, Vanwonterghem I. Understanding the role of micro-organisms in the settlement of coral larvae through community ecology. Mar Biol. 2025;172:43. https://doi.org/10.1007/s00227-025-04607-6.
9. Mason BM, Cohen JH. Long-wavelength photosensitivity in coral planula larvae. Biol Bull. 2012;222:88–92. https://doi.org/10.1086/BBLv222n2p88.
10. Strader ME, Davies SW, Matz MV. Differential responses of coral larvae to the colour of ambient light guide them to suitable settlement microhabitat. R Soc Open Sci. 2015;2:150358. https://doi.org/10.1098/rsos.150358.
11. Mason BM, Koyanagi M, Sugihara T, Iwasaki M, Slepak V, Miller DJ, et al. Multiple opsins in a reef-building coral, *Acropora millepora*. Sci Rep. 2023;13:1628. https://doi.org/10.1038/s41598-023-28476-5.
12. Grasso LC, Maindonald J, Rudd S, Hayward DC, Saint R, Miller DJ, et al. Microarray analysis identifies candidate genes for key roles in coral development. BMC Genomics. 2008;9:1–540. https://doi.org/10.1186/1471-2164-9-540.
13. Hayward DC, Hetherington S, Behm CA, Grasso LC, Forêt S, Miller DJ, et al. Differential gene expression at coral settlement and metamorphosis - a subtractive hybridization study. PLoS ONE. 2011;6:e26411. https://doi.org/10.1371/journal.pone.0026411.
14. Ball EE, Hayward DC, Bridge TCL, Miller DJ. Acropora—The Most-Studied Coral Genus. In: Handbook of Marine Model Organisms in Experimental Biology. CRC Press; 2021. pp. 173–193. CRC Press. https://doi.org/10.1201/9781003217503-10
15. Ball EE, Hayward DC, Reece-Hoyes JS, Hislop NR, Samuel G, Saint R, et al. Coral development: from classical embryology to molecular control. Int J Dev Biol. 2002;46:671–8.
16. Hayward DC, Samuel G, Pontynen PC, Catmull J, Saint R, Miller DJ, et al. Localized expression of a dpp/BMP2/4 ortholog in a coral embryo. Proc Natl Acad Sci U S A. 2002;99:8106–11. https://doi.org/10.1073/pnas.112021499.
17. Ball EE, Hayward DC, Saint R, Miller DJ. A simple plan - cnidarians and the origins of developmental mechanisms. Nat Rev Genet. 2004;5:567–77. https://doi.org/10.1038/nrg1402.
18. Hayward DC, Miller DJ, Ball EE. Snail expression during embryonic development of the coral Acropora: blurring the diploblast/triploblast divide? Dev Genes Evol. 2004;214:257–60. https://doi.org/10.1007/s00427-004-0398-0.
19. Reyes-Bermudez A, Lin Z, Hayward DC, Miller DJ, Ball EE. Differential expression of three galaxin-related genes during settlement and metamorphosis in the scleractinian coral *Acropora millepora*. BMC Evol Biol. 2009;9:178. https://doi.org/10.1186/1471-2148-9-178.
20. Grasso LC, Negri AP, Fôret S, Saint R, Hayward DC, Miller DJ, et al. The biology of coral metamorphosis: molecular responses of larvae to inducers of settlement and metamorphosis. Dev Biol. 2011;353:411–9. https://doi.org/10.1016/j.ydbio.2011.02.010.
21. Meyer E, Davies S, Wang S, Willis B, Abrego D, Juenger T, et al. Genetic variation in responses to a settlement cue and elevated temperature in the reef-building coral *Acropora millepora*. Mar Ecol Prog Ser. 2009;392:81–92. https://doi.org/10.3354/meps08208.
22. Meyer E, Aglyamova GV, Matz MV. Profiling gene expression responses of coral larvae (*Acropora millepora*) to elevated temperature and settlement inducers using a novel RNA-Seq procedure. Mol Ecol. 2011;20:3599–616. https://doi.org/10.1111/j.1365-294X.2011.05205.x.
23. Reyes-Bermúdez A, Rodríguez-Cabal HA. Gene expression microarray analysis during metamorphosis and early calcification in the scleractinian coral Acropora millepora. Invertebr Reprod Dev. 2024;0:1–19. https://doi.org/10.1080/07924259.2024.2401383.
24. Takeuchi T, Yamada L, Shinzato C, Sawada H, Satoh N. Stepwise evolution of coral biomineralization revealed with genome-wide proteomics and transcriptomics. PLoS One. 2016;11:e0156424. https://doi.org/10.1371/journal.pone.0156424.
25. Ishii Y, Hatta M, Deguchi R, Kawata M, Maruyama S. Gene expression alterations from reversible to irreversible stages during coral metamorphosis. Zool Lett. 2022;8:1–11. https://doi.org/10.1186/s40851-022-00187-1.
26. Van Etten J, Shumaker A, Mass T, Putnam HM, Bhattacharya D. Transcriptome analysis provides a blueprint of coral egg and sperm functions. PeerJ. 2020;8:e9739. https://doi.org/10.7717/peerj.9739.
27. Chille E, Strand E, Neder M, Schmidt V, Sherman M, Mass T, et al. Developmental series of gene expression clarifies maternal mRNA provisioning and maternal-to-zygotic transition in a reef-building coral. BMC Genomics. 2021;22:815. https://doi.org/10.1186/s12864-021-08114-y.
28. Mansour TA, Rosenthal JJC, Brown CT, Roberson LM. Transcriptome of the Caribbean stony coral *Porites astreoides* from three developmental stages. Gigascience. 2016;5:s13742-016-0138–1. https://doi.org/10.1186/s13742-016-0138-1.
29. Walker NS, Fernández R, Sneed JM, Paul VJ, Giribet G, Combosch DJ. Differential gene expression during substrate probing in larvae of the Caribbean coral *Porites astreoides*. Mol Ecol. 2019;28:4899–913. https://doi.org/10.1111/mec.15265.
30. Huffmyer AS, Wong KH, Becker DM, Strand E, Mass T, Putnam HM. Shifts and critical periods in coral metabolism reveal energetic vulnerability during development. Curr Biol. 2025;35:2858-2871.e6. https://doi.org/10.1016/j.cub.2025.05.013.
31. Levy S, Elek A, Grau-Bové X, Menéndez-Bravo S, Iglesias M, Tanay A, et al. A stony coral cell atlas illuminates the molecular and cellular basis of coral symbiosis, calcification, and immunity. Cell. 2021;184:2973-2987.e18. https://doi.org/10.1016/j.cell.2021.04.005.
32. Gilbert E, Craggs J, Modepalli V. Gene regulatory network that shaped the evolution of larval apical organ in cnidaria. Mol Biol Evol. 2024;41:msad285. https://doi.org/10.1093/molbev/msad285.
33. Ramon-Mateu J, Ferraioli A, Teixidó N, Domart-Coulon I, Houliston E, Copley RR. Aboral cell types of *Clytia* and coral larvae have shared features and link taurine to the regulation of settlement. Sci Adv. 2025;11:eadv1159. https://doi.org/10.1126/sciadv.adv1159.
34. Reyes-Bermudez A, Villar-Briones A, Ramirez-Portilla C, Hidaka M, Mikheyev AS. Developmental progression in the coral *Acropora digitifera* is controlled by differential expression of distinct regulatory gene networks. Genome Biol Evol. 2016;8:851–70. https://doi.org/10.1093/gbe/evw042.
35. Allemand D, Tambutté É, Zoccola D, Tambutté S. Coral Calcification, Cells to Reefs. In: Dubinsky Z, Stambler N, editors. Coral Reefs: An Ecosystem in Transition. Dordrecht: Springer Netherlands; 2011. pp. 119–50. https://doi.org/10.1007/978-94-007-0114-4_9.
36. Akiva A, Neder M, Kahil K, Gavriel R, Pinkas I, Goobes G, et al. Minerals in the pre-settled coral *Stylophora pistillata* crystallize via protein and ion changes. Nat Commun. 2018;9:1880. https://doi.org/10.1038/s41467-018-04285-7.
37. Neder M, Laissue PP, Akiva A, Akkaynak D, Albéric M, Spaeker O, et al. Mineral formation in the primary polyps of pocilloporoid corals. Acta Biomater. 2019;96:631–45. https://doi.org/10.1016/j.actbio.2019.07.016.
38. Langfelder P, Horvath S. WGCNA: an R package for weighted correlation network analysis. BMC Bioinformatics. 2008;9:559. https://doi.org/10.1186/1471-2105-9-559.
39. Ayers TN, Nicotra ML, Lee MT. Parallels and contrasts between the cnidarian and bilaterian maternal-to-zygotic transition are revealed in Hydractinia embryos. PLoS Genetics 2023;19(7):e1010845.
40. Michail C, Rodrigues Lima F, Viguier M, Deshayes F. Structure and function of the lysine methyltransferase SETD2 in cancer: from histones to cytoskeleton. Neoplasia. 2025;59:101090. https://doi.org/10.1016/j.neo.2024.101090.
41. Technau U. Gastrulation and germ layer formation in the sea anemone *Nematostella vectensis* and other cnidarians. Mech Dev. 2020;163:103628. https://doi.org/10.1016/j.mod.2020.103628.
42. Hayward DC, Grasso LC, Saint R, Miller DJ, Ball EE. The organizer in evolution–gastrulation and organizer gene expression highlight the

importance of Brachyury during development of the coral, Acropora millepora. Dev Biol. 2015;399:337–47. https://doi.org/10.1016/j.ydbio.2015.01.006.

43. Yasuoka Y, Shinzato C, Satoh N. The mesoderm-forming gene brachyury regulates ectoderm-endoderm demarcation in the coral Acropora digitifera. Curr Biol. 2016;26:2885–92. https://doi.org/10.1016/j.cub.2016.08.011.
44. Okubo N, Mezaki T, Nozawa Y, Nakano Y, Lien Y-T, Fukami H, et al. Comparative embryology of eleven species of stony corals (Scleractinia). PLoS ONE. 2013;8:e84115. https://doi.org/10.1371/journal.pone.0084115.
45. Okubo N, Hayward DC, Forêt S, Ball EE. A comparative view of early development in the corals Favia lizardensis, Ctenactis echinata, and Acropora millepora - morphology, transcriptome, and developmental gene expression. BMC Evol Biol. 2016;16:48. https://doi.org/10.1186/s12862-016-0615-2.
46. Mason B, Cooke I, Moya A, Augustin R, Lin M-F, Satoh N, et al. AmAMP1 from *Acropora millepora* and damicornin define a family of coral-specific antimicrobial peptides related to the Shk toxins of sea anemones. Dev Comp Immunol. 2021;114:103866. https://doi.org/10.1016/j.dci.2020.103866.
47. Miller DJ, Hemmrich G, Ball EE, Hayward DC, Khalturin K, Funayama N, et al. The innate immune repertoire in Cnidaria - ancestral complexity and stochastic gene loss. Genome Biol. 2007;8:R59. https://doi.org/10.1186/gb-2007-8-4-r59.
48. Mason B, Hayward DC, Moya A, Cooke I, Sorenson A, Brunner R, et al. Microbiome manipulation by corals and other Cnidaria via quorum quenching. Curr Biol. 2024;34:3226-3232.e5. https://doi.org/10.1016/j.cub.2024.05.073.
49. Hadfield MG. Why and how marine-invertebrate larvae metamorphose so fast. Semin Cell Dev Biol. 2000;11:437–43. https://doi.org/10.1006/scdb.2000.0197.
50. Mishima Y, Tomari Y. Pervasive yet nonuniform contributions of Dcp2 and Cnot7 to maternal mRNA clearance in zebrafish. Genes Cells. 2017;22:670–8. https://doi.org/10.1111/gtc.12504.
51. Baugh LR, Hill AA, Slonim DK, Brown EL, Hunter CP. Composition and dynamics of the Caenorhabditis elegans early embryonic transcriptome. Development. 2003;130:889–900. https://doi.org/10.1242/dev.00302.
52. Mohr F, Döhner K, Buske C, Rawat VPS. TET genes: new players in DNA demethylation and important determinants for stemness. Exp Hematol. 2011;39:272–81. https://doi.org/10.1016/j.exphem.2010.12.004.
53. Wu X, Zhang Y. TET-mediated active DNA demethylation: mechanism, function and beyond. Nat Rev Genet. 2017;18:517–34. https://doi.org/10.1038/nrg.2017.33.
54. Jessop P, Ruzov A, Gering M. Developmental functions of the dynamic DNA methylome and hydroxymethylome in the mouse and zebrafish: similarities and differences. Front Cell Dev Biol. 2018;6:27. https://doi.org/10.3389/fcell.2018.00027.
55. Gerber AP, Luschnig S, Krasnow MA, Brown PO, Herschlag D. Genome-wide identification of mRNAs associated with the translational regulator PUMILIO in Drosophila melanogaster. Proc Natl Acad Sci U S A. 2006;103:4487–92. https://doi.org/10.1073/pnas.0509260103.
56. Rabani M, Pieper L, Chew G-L, Schier AF. A massively parallel reporter assay of 3′ UTR sequences identifies in vivo rules for mRNA degradation. Mol Cell. 2017;68:1083-1094.e5. https://doi.org/10.1016/j.molcel.2017.11.014.
57. Chen L, Dumelie JG, Li X, Cheng MH, Yang Z, Laver JD, et al. Global regulation of mRNA translation and stability in the early Drosophilaembryo by the Smaug RNA-binding protein. Genome Biol. 2014;15:R4. https://doi.org/10.1186/gb-2014-15-1-r4.
58. Spike CA, Tsukamoto T, Greenstein D. Ubiquitin ligases and a processive proteasome facilitate protein clearance during the oocyte-to-embryo transition in Caenorhabditis elegans. Genetics. 2022;221:iyac051. https://doi.org/10.1093/genetics/iyac051.
59. Aviv T, Lin Z, Lau S, Rendl LM, Sicheri F, Smibert CA. The RNA-binding SAM domain of Smaug defines a new family of post-transcriptional regulators. Nat Struct Biol. 2003;10:614–21. https://doi.org/10.1038/nsb956.
60. Bartel DP. MicroRNAs: genomics, biogenesis, mechanism, and function. Cell. 2004;116:281–97. https://doi.org/10.1016/S0092-8674(04)00045-5.
61. Praher D, Zimmermann B, Genikhovich G, Columbus-Shenkar Y, Modepalli V, Aharoni R, et al. Characterization of the piRNA pathway during development of the sea anemone Nematostella vectensis. RNA Biol. 2017;14:1727–41. https://doi.org/10.1080/15476286.2017.1349048.
62. Moran Y, Agron M, Praher D, Technau U. The evolutionary origin of plant and animal microRNAs. Nat Ecol Evol. 2017;1:0027. https://doi.org/10.1038/s41559-016-0027.
63. Modepalli V, Fridrich A, Agron M, Moran Y. The methyltransferase HEN1 is required in *Nematostella vectensis* for microRNA and piRNA stability as well as larval metamorphosis. PLoS Genet. 2018;14:e1007590. https://doi.org/10.1371/journal.pgen.1007590.
64. Fridrich A, Modepalli V, Lewandowska M, Aharoni R, Moran Y. Unravelling the developmental and functional significance of an ancient argonaute duplication. Nat Commun. 2020;11:6187. https://doi.org/10.1038/s41467-020-20003-8.
65. Bamberger C, Pankow S, Yates JR. Nvp63 and nvPIWIL1 suppress retrotransposon activation in the sea anemone *Nematostella vectensis*. J Proteome Res. 2022;21:2586–95. https://doi.org/10.1021/acs.jproteome.2c00296.
66. Matsumoto N, Sato K, Nishimasu H, Namba Y, Miyakubi K, Dohmae N, et al. Crystal structure and activity of the endoribonuclease domain of the piRNA pathway factor Maelstrom. Cell Rep. 2015;11:366–75. https://doi.org/10.1016/j.celrep.2015.03.030.
67. Sato K, Siomi MC. Functional and structural insights into the piRNA factor Maelstrom. FEBS Lett. 2015;589:1688–93. https://doi.org/10.1016/j.febslet.2015.03.023.
68. Rocchini C, Marx RM, von Schnorr Carosfeld J, Kasinsky HE, Rosenberg E, Sommer F, et al. Replacement of nucleosomal histones by histone H1-like proteins during spermiogenesis in Cnidaria: evolutionary implications. J Mol Evol. 1996;42:240–6. https://doi.org/10.1007/BF02198850.
69. Török A, Schiffer PH, Schnitzler CE, Ford K, Mullikin JC, Baxevanis AD, et al. The cnidarian *Hydractinia echinata* employs canonical and highly adapted histones to pack its DNA. Epigenetics Chromatin. 2016;9:36. https://doi.org/10.1186/s13072-016-0085-1.
70. Lorković ZJ, Berger F. Heterochromatin and DNA damage repair: use different histone variants and relax. Nucleus. 2017;8:583–8. https://doi.org/10.1080/19491034.2017.1384893.
71. Herchenröther A, Wunderlich TM, Lan J, Hake SB. Spotlight on histone H2A variants: from b to x to z. Semin Cell Dev Biol. 2023;135:3–12. https://doi.org/10.1016/j.semcdb.2022.03.025.
72. Osakabe A, Molaro A. Histone renegades: unusual H2A histone variants in plants and animals. Semin Cell Dev Biol. 2023;135:35–42. https://doi.org/10.1016/j.semcdb.2022.05.001.
73. Iwao K, Fujisawa T, Hatta M. A cnidarian neuropeptide of the GLWamide family induces metamorphosis of reef-building corals in the genus *Acropora*. Coral Reefs. 2002;21:127–9.
74. Attenborough RMF, Hayward DC, Wiedemann U, Forêt S, Miller DJ, Ball EE. Expression of the neuropeptides RFamide and LWamide during development of the coral *Acropora millepora* in relation to settlement and metamorphosis. Dev Biol. 2019;446:56–67. https://doi.org/10.1016/j.ydbio.2018.11.022.
75. Vastenhouw NL, Cao WX, Lipshitz HD. The maternal-to-zygotic transition revisited. Development. 2019;146:dev161471. https://doi.org/10.1242/dev.161471.
76. Aeschimann F, Neagu A, Rausch M, Großhans H. Let-7 coordinates the transition to adulthood through a single primary and four secondary targets. Life Sci Alliance. 2019. https://doi.org/10.26508/lsa.201900335.
77. Mazza ME, Pang K, Reitzel AM, Martindale MQ, Finnerty JR. A conserved cluster of three PRD-class homeobox genes (homeobrain, rx and orthopedia) in the Cnidaria and Protostomia. EvoDevo. 2010;1:3. https://doi.org/10.1186/2041-9139-1-3.
78. Hadfield MG. Biofilms and marine invertebrate larvae: what bacteria produce that larvae use to choose settlement sites. Annu Rev Mar Sci. 2011;3:453–70.
79. Tran C, Hadfield MG. Are G-protein-coupled receptors involved in mediating larval settlement and metamorphosis of coral planulae? Biol Bull. 2012;222:128–36. https://doi.org/10.1086/bblv222n2p128.
80. Morse DE, Hooker N, Morse ANC, Jensen RA. Control of larval metamorphosis and recruitment in sympatric agariciid corals. J Exp Mar Biol Ecol. 1988;116:193–217. https://doi.org/10.1016/0022-0981(88)90027-5.

81. Negri AP, Webster N, Hill R, Heyward A. Metamorphosis of broadcast spawning corals in response to bacteria isolated from crustose algae. Mar Ecol Prog Ser. 2001;223:121–31. https://doi.org/10.3354/meps223121.
82. Kitamura M, Koyama T, Nakano Y, Uemura D. Characterization of a natural inducer of coral larval metamorphosis. J Exp Mar Biol Ecol. 2007;340:96–102. https://doi.org/10.1016/j.jembe.2006.08.012.
83. Birrell C, McCook L, Willis B, Harrington L. Chemical effects of macroalgae on larval settlement of the broadcast spawning coral Acropora millepora. Mar Ecol Prog Ser. 2008;362:129–37. https://doi.org/10.3354/meps07524.
84. Kitamura M, Schupp PJ, Nakano Y, Uemura D. Luminaolide, a novel metamorphosis-enhancing macrodiolide for scleractinian coral larvae from crustose coralline algae. Tetrahedron Lett. 2009;50:6606–9. https://doi.org/10.1016/j.tetlet.2009.09.065.
85. Whitman TN, Negri AP, Bourne DG, Randall CJ. Settlement of larvae from four families of corals in response to a crustose coralline alga and its biochemical morphogens. Sci Rep. 2020;10:16397. https://doi.org/10.1038/s41598-020-73103-2.
86. Russell DW, Sambrook J. Molecular cloning: a laboratory manual. Cold Spring Harbor: Cold Spring Harbor Laboratory; 2001.
87. Di Tommaso P, Chatzou M, Floden EW, Barja PP, Palumbo E, Notredame C. Nextflow enables reproducible computational workflows. Nat Biotechnol. 2017;35:316–9. https://doi.org/10.1038/nbt.3820.
88. Breitwieser FP, Baker DN, Salzberg SL. KrakenUniq: confident and fast metagenomics classification using unique k-mer counts. Genome Biol. 2018;19:198. https://doi.org/10.1186/s13059-018-1568-0.
89. Chen S, Zhou Y, Chen Y, Gu J. Fastp: an ultra-fast all-in-one FASTQ preprocessor. Bioinformatics. 2018;34:i884. https://doi.org/10.1093/bioinformatics/bty560.
90. Shoguchi E, Beedessee G, Hisata K, Tada I, Narisoko H, Satoh N, et al. A new dinoflagellate genome illuminates a conserved gene cluster involved in sunscreen biosynthesis. Genome Biol Evol. 2021;13:evaa235. https://doi.org/10.1093/gbe/evaa235.
91. Langmead B, Salzberg SL. Fast gapped-read alignment with Bowtie 2. Nat Methods. 2012;9:357–9. https://doi.org/10.1038/nmeth.1923.
92. Li B, Dewey CN. RSEM: accurate transcript quantification from RNA-Seq data with or without a reference genome. BMC Bioinformatics. 2011;12:323. https://doi.org/10.1186/1471-2105-12-323.
93. Love MI, Huber W, Anders S. Moderated estimation of fold change and dispersion for RNA-seq data with DESeq2. Genome Biol. 2014;15:550. https://doi.org/10.1186/s13059-014-0550-8.
94. Jones P, Binns D, Chang H-Y, Fraser M, Li W, McAnulla C, et al. InterProScan 5: genome-scale protein function classification. Bioinformatics. 2014;30:1236–40. https://doi.org/10.1093/bioinformatics/btu031.
95. R Core Team. R: A Language and Environment for Statistical Computing. 2024. https://www.r-project.org/. Accessed 10 Mar 2025.
96. Chang W, Cheng J, Allaire JJ, Sievert C, Schloerke B, Xie Y, et al. shiny: Web Application Framework for R. 2024.
97. Wickham H. Data Analysis. In: Wickham H, editor. ggplot2: Elegant Graphics for Data Analysis. Cham: Springer International Publishing; 2016. pp. 189–201. https://doi.org/10.1007/978-3-319-24277-4_9.
98. Gu Z, Hübschmann D. Make interactive complex heatmaps in R. Bioinformatics. 2022;38:1460–2. https://doi.org/10.1093/bioinformatics/btab806.
99. Hayward DC, Catmull J, Reece-Hoyes JS, Berghammer H, Dodd H, Hann SJ, et al. Gene structure and larval expression of cnox-2Am from the coral *Acropora millepora*. Dev Genes Evol. 2001;211:10–9. https://doi.org/10.1007/s004270000112.
100. Kucharski R, Ball EE, Hayward DC, Maleszka R. Molecular cloning and expression analysis of a cDNA encoding a glutamate transporter in the honeybee brain. Gene. 2000;242:399–405. https://doi.org/10.1016/S0378-1119(99)00503-X.
101. Rosen B, Beddington RSP. Whole-mount in situ hybridization in the mouse embryo: gene expression in three dimensions. Trends Genet. 1993;9:162–7. https://doi.org/10.1016/0168-9525(93)90162-B.

Publisher's Note